SSRG International Journal of Electrical and Electronics Engineering
ISSN: 2348-8379/ https://doi.org/10.14445/23488379/IJEEE-V13I7P101

Volume 13 Issue 7, 1-40, July 2026

Original Article

Analysis in the Nonlinear Region of a MOSFET using Physical Characteristics and the BSIM4 Library

Fredy Javier Vilca Zamata[1], German Alberto Echaiz Espinoza[2], Clara Alheli Quispe Mamani[3], Ines Roxana Cayllahua Chire[3], Pedro Alberto Mamani Apaza[4], Carmelo Mayta Ojeda[5], Fernando Enrique Echaiz Espinoza[6]

[1,3]*School of Electronic Engineering, National University of San Agustín de Arequipa, Arequipa, Peru.*
[2]*Academic Department of Electronic Engineering, National University of San Agustín de Arequipa, Arequipa, Peru.*
[4]*Academic Department of Mathematics, Universidad Nacional de San Agustín de Arequipa, Arequipa, Perú.*
[5]*Academic Department of Physics, National University of San Agustín de Arequipa, Arequipa, Peru.*
[6]*Institute of Mathematics, Federal University of Alagoas, Maceio, Brazil.*

[2]*Corresponding Author : gechaiz@unsa.edu.pe*

Received: 21 July 2025 Revised: 13 September 2025 Accepted: 19 June 2026 Published: 27 July 2026

Abstract *- This paper the nonlinear response of a 65 nm MOSFET in moderate inversion and saturation regions is analyzed through a mathematical formulation. Harmonic components are derived from the drain current expression by employing modified Bessel functions. These results are compared with numerical simulations performed in the NGSpice environment using the BSIM4 library. The simulations allow us to verify the appearance and magnitude of the harmonics found analytically. In addition, the analysis is replicated using MATLAB, facilitating parametric evaluation and detailed visualization of the current harmonic. The bias conditions are also analyzed to minimize unwanted harmonics, for which criteria are evaluated that allow the design of analog circuits with low distortion. Finally, all associated codes and findings have been made available to the public in an online repository.*

Keywords *- NGSpice, BSIM4, MOSFET, Modified Bessel Functions, Nonlinear Analysis.*

1. Introduction

The moderate inversion regime has attracted considerable attention due to its transitional behavior between weak and strong inversion, as discussed by Tsividis in [1, 14]. Throughout the years, numerous scholars have introduced models designed to precisely capture how drain current varies in response to gate and drain voltages. The "reconciliation" model created by Tsividis, Suyama, and Vavelidis is an important contribution to this field [7].

These early insights laid the groundwork for subsequent research on linearity in the moderate inversion regime, notably studies by Van Langevelde and Klaasen [2] and Toole, Plett, and Cloutier [3], who pinpointed specific operating points, commonly referred to as sweet spots, where harmonic distortion is minimized. However, these theoretical frameworks were constructed on idealized or simplified premises, frequently neglecting the intricate physical phenomena inherent in nanoscale technologies.

The BSIM4 model, which is now part of simulation platforms like NGSpice [12], made it possible to show how transistors behave more accurately by taking into account things like channel modulation, contact resistance, and variations in carrier mobility [11]. This progress has given scholars new chances to look at and build on what they have already learned. This study serves as both a replication and an extension of the reconciliation model introduced by Igor M.

Filanovsky in [13], which is based on the use of modified Bessel functions to analyze the nonlinear behavior of MOS transistors. Its aim is to validate theoretical forecasts regarding second and third order harmonic distortion in 65 nm MOSFET devices while simultaneously broadening the scope by integrating simulations based on the BSIM4 physical model alongside computations using modified Bessel functions. By combining these analytical and numerical techniques, the research offers enhanced insights into the nonlinear characteristics of MOSFETs operating in moderate inversion and saturation regions, ultimately providing useful guidelines for designing amplifiers with minimal distortion [10].

Section III describes the formulation of the proposed model for MOSFET operation in moderate inversion and strong saturation. The proposed model is further contrasted with the g_m/I_D approach described in [4, 5]. Section IV covers the key properties of modified Bessel functions that are necessary for harmonic computations [13].

Section V examines the harmonic behavior produced by gate to source and drain to source voltage variations, together with the intermodulation components generated when both excitations are simultaneously applied. You can also get the formulas you need to figure out these harmonics. Section VI is a real-world example of how to look at the harmonic distortion in a common-source amplifier. This part further looks into how changes in the transistor's threshold voltage effect the suppression of second and third order harmonic components. It also gives advice on how to choose the best gate-bias voltage.

Section VII analyzes the impact of drain terminal variations on the appropriate. V_{DS} operating condition. Section VIII further develops the harmonic analysis by determining the 1dB compression point and by assessing the contribution of modified Bessel functions to the characterization of nonlinear behavior. Finally, Section IX gives a brief summary of the main results and stresses the main conclusions that may be drawn from the research.

2. Methodology

This research employs a replication and extension methodology to validate the theoretical results reported by Igor M. Filanovsky and Oliveira in [6, 13], concerning the computation of harmonic components in MOS transistors operating in the moderate inversion region. Furthermore, the study extends this analytical framework by incorporating physical simulations based on the BSIM4 model in NGSpice, with additional computational validation performed in MATLAB.

2.1. The Overall Design

Both analytical and numerical methods are used in this investigation.

- During the replication stage, the calculation of second and third order harmonics was repeated using analytical expressions that used series expansions of modified Bessel functions [6].
- During the extension stage, the BSIM4 model was used in the NGSpice platform to run simulations of a 65 nm MOSFET transistor. This made it possible to compare what the theory said would happen with what actually happened.

2.2. Parameters of the Device

The 65 nm NMOS transistor that is being looked at has certain characteristics, such as threshold voltage ($V_{TH} = 0.24V$), a substrate factor of $n = 1.3$, thermal voltage ($\phi_t = 0.0250V$), and the ratio of width to length ($W/L = 50/65\ \mu m$). These parameters were selected based on the guidelines provided in the BSIM4 manual [11].

2.3. Tools for Simulations

The $besseli(n, x)$ functions in MATLAB were used to repeat theoretical harmonic computations for A_2 and A_3 and to show the normalized results. NGSpice was used to model how the transistor will function under different bias situations and to find harmonic components by using FFT analysis on the drain signal [12]. Python was a useful tool that helped with automating voltage sweep methods and handling the data that NGSpice generated for more investigation.

2.4. Steps

The theoretical reconciliation model was coded in MATLAB, using a logarithmic expansion that was cut off to only include exponential and algebraic parts. We did calculations of the second and third order harmonics for different signal amplitudes and biasing settings. In NGSpice, a netlist with the BSIM4 model was made to recreate these conditions.

Next, an FFT analysis was done on the drain current in relation to the gate voltage, and the results were compared to what was expected based on theory. Finally, the effect of changes in threshold voltage on distortion was looked at. This led to the discovery of the best bias points, known as "sweet spots", that help lower harmonic and intermodulation distortions.

3. New Transistor Model

The behavior of the MOSFET between the inversion and moderate saturation regions can't be described by a single simplified analytical expression. Models based on separate equations for different operating regions tend to be inaccurate when approaching the transition limits.

For this reason, expressions have been developed that guarantee continuity under all operating conditions. When the body effect is not considered in an n-channel transistor, the drain current I_D may be described by the reconciliation model, as shown below:

$$I_D = I_{ref}\left[ln^2\left(1 + e^{\frac{V_{GS}-V_{TH}}{2n\phi_t}}\right) - ln^2\left(1 + e^{\frac{V_{GS}-V_{TH}-nV_{DS}}{2n\phi_t}}\right)\right] \tag{1}$$

The thermal Voltage, denoted as ϕ_t, corresponds to the ratio kT/q. In addition, V_{TH} represents the threshold voltage, and I_{ref} is introduced as the reference current $\left(2\,\mu\,C'_{ox}\left(\frac{W}{L}\right)n\phi_t^2\right)$. According to the approximation in [7], the substrate factor n can be estimated as $n \approx 1 + \left[\gamma/\left(2\sqrt{V_{SB} + 2\phi_F}\right)\right]$, where ϕ_F represents the Fermi potential, and γ is the body effect coefficient. In this formulation, all voltages are referenced relative to the source terminal.

The formulation isolates a contribution associated exclusively with V_{GS} (inversion) from another contribution that depends on both V_{GS} and V_{DS}. When V_{DS} reaches sufficiently high values, its contribution may be neglected, and the drain current I_D is governed by the difference $V_{GS} - V_{TH}$ together with a V_{DS}. Furthermore, V_{TH}, ϕ_t, and n are positive constants for all MOS transistors ($V_{TH} > 0, \phi_t > 0, n > 0$)

$$nV_{DS} \gg V_{GS} - V_{TH}$$

$$0 \gg \frac{V_{GS}-V_{TH}-nV_{DS}}{2n\phi_t}$$

then

$$e^{\frac{V_{GS}-V_{TH}-nV_{DS}}{2n\phi_t}} \rightarrow 0$$

The current can be roughly equal to the following:

$$I_D = I_{ref}\left[ln^2\left(1+e^{\frac{V_{GS}-V_{TH}}{2n\phi_t}}\right)\right] \tag{2}$$

from (2), it is obtained that

$$\frac{g_m}{I_D} = \frac{\sqrt{I_{ref}/I_D}}{n\phi_t}\left(1-\frac{1}{e^{\sqrt{I_D/I_{ref}}}}\right) \tag{3}$$

where $g_m = \frac{\partial I_D}{\partial V_{GS}}$.

When V_{GS} and V_{DS} include sinusoidal variations, Equations (1) and (2) do not effectively capture nonlinear distortion effects. To facilitate further analysis, it is useful to employ two series expansions of logarithmic functions, which are as follows [10] (the supporting proofs are available in the appendix section):

$$ln^2(x) = \left[ln(x-1) - \sum_{n=1}^{\infty}\frac{(-1)^n}{(x-1)^n n}\right]^2 \tag{4}$$

for $|x-1| > 1$, and

$$ln^2(x) = \left[\sum_{n=1}^{\infty}\frac{(-1)^n(x-1)^n}{n}\right]^2 \tag{5}$$

for $|x-1| < 1$.

By utilizing two terms from Equation (4) with $\left(x = 1 + e^{\frac{V_{GS}-V_{TH}}{2n\phi_t}}\right)$ and two terms from Equation (5) with $\left(x = 1 + e^{\frac{V_{GS}-V_{TH}-nV_{DS}}{2n\phi_t}}\right)$ while modifying the coefficients α_1 and α_2 In the latter, as detailed in [8], a revised model can be formulated. This model is applicable to the moderate inversion region where ($V_{GS} > V_{TH}$) and to the saturation region characterized by ($|V_{GS} - V_{TH}| \leq |n\,V_{DS}|$):

$$I_{out} = I_{ref}\left[\begin{array}{l}\left(e^{-\frac{V_{GS}-V_{TH}}{2n\phi_t}} + \frac{V_{GS}-V_{TH}}{2n\phi_t} - \alpha_1 e^{-\frac{V_{GS}-V_{TH}}{n\phi_t}}\right)^2 \\ -e^{\frac{V_{GS}-V_{TH}-nV_{DS}}{n\phi_t}}\left(1-\alpha_2 e^{\frac{V_{GS}-V_{TH}-nV_{DS}}{2n\phi_t}}\right)\end{array}\right] \tag{6}$$

In this context, α_1 is defined as $1 - ln2$, and α_2 as $1 - (ln2)^2$. The symbol I_{out} denotes the drain current corresponding to the moderate inversion and saturation regions, with condition (2) suggested to be called deep saturation. Based on this, model (6) can be simplified by excluding the terms involving, $\alpha_1$and, α_2, resulting in a more concise equation presented below:

$$I_{out} = I_{ref}\left[\left(e^{-\frac{V_{GS}-V_{TH}}{2n\phi_t}} + \frac{V_{GS}-V_{TH}}{2n\phi_t}\right)^2 - e^{\frac{V_{GS}-V_{TH}-nV_{DS}}{n\phi_t}}\right] \tag{7}$$

The excluded terms help create a seamless and gradual transition between neighboring operating regions, such as weak, moderate, and strong inversion and across different saturation levels. Although these terms are exponential and do not impact the methods used for harmonic analysis, incorporating them would unnecessarily complicate the outcomes without improving alignment with simulation data.

Equation (7) shows that the combined contribution of the first two components, including their squared interaction, describes the transition between moderate and strong inversion [8].

The remaining component becomes significant under the condition. ($|V_{GS} - V_{TH}| < |n\,V_{DS}|$) , corresponding to the strong saturation region. This contribution also plays a key role in determining the output impedance of the transistor.

$$g_{out} = \frac{\partial}{\partial V_{DS}}\left(-I_{ref}e^{\frac{V_{GS}-V_{TH}-nV_{DS}}{n\phi_t}}\right) = \frac{I_{ref}}{\phi_t}e^{\frac{V_{GS}-V_{TH}-nV_{DS}}{n\phi_t}} \tag{8}$$

In this context, Equation (7) is used to compute harmonics components in the common source (CS) stage (see Figure 1). The input and output voltages are assumed to contain sinusoidal signals, expressed as by $v_{gs} = V_{gm}\,cos(\omega t)$ and $v_{ds} = V_{dm}\,cos(\Omega t)$.

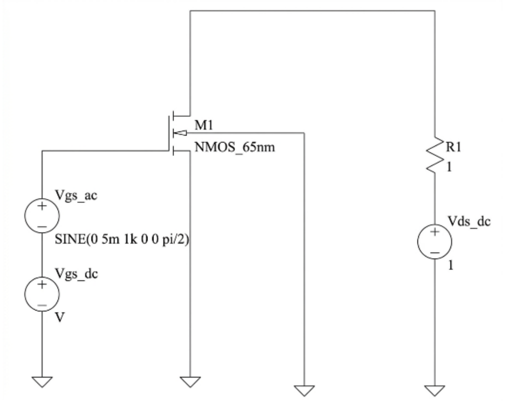

Fig. 1 Common source configuration subject to simultaneous modulation at the gate and drain terminals.

4. Modified Bessel Functions

Modified Bessel functions play a key role in the analysis of nonlinear phenomena. For a given order n and argument x, they can be introduced through an integral representation of the following form [9]:

$$I_n(x) = \frac{1}{2\pi}\int_{-\pi}^{\pi} e^{x cos\theta} cos n\theta \ d\theta.$$

Before representing $I_n(x)$ Through a Fourier expansion, it is necessary to verify both its periodicity and integrability. To find harmonics, you need to use certain arithmetic formulas [9, 13] that use modified Bessel functions.

$$e^{x\, cos(\omega t)} = I_0(x) + 2\sum_{n=1}^{\infty} I_n\,(x)\,cos(\,n\omega t) \qquad (9)$$

$$e^{-x\, cos(\omega t)} = I_0(x) + 2\sum_{n=1}^{\infty}(-1)^n I_n\,(x)\,cos(\,n\omega t) \qquad (10)$$

The terms $I_n(x)$, including $I_0(x), I_1(x), ...$, correspond to modified Bessel functions of the first kind [9, 16]. You can get these in MATLAB by using the command $besseli(n, x)$. You can also use the series expansion below to find them. The corresponding solution of the modified Bessel equation of the first kind is given by:

$$I_n(x) = \sum_{p=0}^{\infty} \frac{1}{k!\Gamma(p+n+1)}\left(\frac{x}{2}\right)^{2p+n} \qquad (11)$$

The expanded form of the preceding summation leads directly to the series representation reported in [13]. Since this development follows from the general expression above, it is omitted here for brevity. Approximate numerical values associated with the resulting series can be found in [9]. For positive integer values, the gamma function $\Gamma(p)$ is equal to $(p-1)!$.

$$I_0(x) \approx 1 + \frac{x^2}{4}, I_1(x) \approx \frac{x}{2} + \frac{x^3}{16}, I_2(x) \approx \frac{x^2}{8}, I_3(x) \approx \frac{x^3}{48} \quad (12)$$

From the approximations above, we can see a pattern: for orders $n \geq 1$, the leading term of the modified Bessel function scales as $\frac{\left(\frac{x}{2}\right)^n}{n!}$. This discovery leads to the general approximation. $I_n(x) \approx \ (x/2)^n/n!$. Also, keep in mind that the amplitudes of the modified Bessel functions drop down quickly as the order goes up, even if the argument stays the same. This trait is quite helpful when you need to figure out which intermodulation component is probably the most relevant.

5. Calculation of the Harmonics of I_D.

Assume that the gate to source voltage includes a sinusoidal component, so that. $V_{GS} = V_{GS0} + V_{gm}cos(\omega t)$. Within this framework, we define the normalized variables $X = \frac{V_{GS0} - V_{TH}}{2n\,\phi_t}$ and $x = \frac{V_{gm}}{2n\,\phi_t}$.

Likewise, when the drain to source voltage contains a sinusoidal element, it can be represented as $V_{DS} = V_{DS0} + V_{dm}cos(\Omega t)$. Under these conditions, the normalized variables are defined as $Y = \frac{V_{GS0} - V_{TH} - n\,V_{DS0}}{n\phi_t}$ and $y = \frac{V_{dm}}{\phi_t}$, adapted from [13].

$$I_{out} = I_{ref}\left[\left(e^{-\frac{V_{GS}-V_{TH}}{2n\phi_t}} + \frac{V_{GS}-V_{TH}}{2n\phi_t}\right)^2 - e^{\frac{V_{GS}-V_{TH}-nV_{DS}}{n\phi_t}}\right]$$

Substituting the previously mentioned equations into Equation (7), we obtain the following:

$$I_{out} = I_{ref}\left[\begin{array}{l}\left(e^{-\frac{V_{GS0}+V_{gm}\,cos(\omega t)-V_{TH}}{2n\phi_t}} + \frac{V_{GS0}+V_{gm}\,cos(\omega t)-V_{TH}}{2n\phi_t}\right)^2 \\ -e^{\frac{V_{GS0}+V_{gm}\,cos(\omega t)-V_{TH}-n(V_{DS0}+V_{dm}\,cos(\Omega t))}{n\phi_t}}\end{array}\right]$$

By rearranging, it would result in

$$I_{out} = I_{ref}\left[\begin{array}{l}\left(e^{-\left(\frac{V_{GS0}-V_{TH}}{2n\phi_t}+\frac{V_{gm}}{2n\phi_t}cos(\omega t)\right)} + \frac{V_{GS0}-V_{TH}}{2n\phi_t} + \frac{V_{gm}}{2n\phi_t}cos(\,\omega t)\right)^2 \\ -e^{\frac{V_{GS0}-V_{TH}-nV_{DS0}}{n\phi_t}+\frac{2V_{gm}}{2n\phi_t}cos(\omega t)-\frac{V_{dm}}{\phi_t}cos(\Omega t)}\end{array}\right]$$

By applying these normalized variables, Equation (7) may be reformulated as follows:

$$I_{out} = I_{ref}\left\{\begin{matrix}\left(e^{-(X+x\cos(\omega t))} + X + x\cos(\omega t)\right)^2 - \\ e^{(Y+2x\cos(\omega t) - y\cos(\Omega t))}\end{matrix}\right\} \tag{13}$$

Using the approximation introduced in [13]:

$$e^{-x\cos(\omega t)} \approx I_0(x) - 2I_1(x)\cos(\omega t) + 2I_2(x)\cos(2\omega t) - 2I_3(x)\cos(3\omega t) \tag{14}$$

$$e^{-2x\cos(\omega t)} \approx I_0(2x) - 2I_1(2x)\cos(\omega t) + 2I_2(2x)\cos(2\omega t) - 2I_3(2x)\cos(3\omega t) \tag{15}$$

and

$$e^{-y\cos(\Omega t)} \approx I_0(y) - 2I_1(y)\cos(\Omega t) + 2I_2(y)\cos(2\Omega t) - 2I_3(y)\cos(3\Omega t) \tag{16}$$

The analysis reveals that:

$$I_{out} = I_G + I_D \tag{17}$$

$$I_{out} = \underbrace{I_{ref}\left\{X + x\cos(\omega t) + e^{-(X - x\cos(\omega t))}\right\}^2}_{I_G} + \underbrace{I_{ref}\left\{-e^{(Y+2x\cos(\omega t) - y\cos(\Omega t))}\right\}}_{I_D}$$

The term I_G is expanded, and using approximations (14) and (15), we obtain the following:

$$I_G = I_{ref}\left\{\begin{matrix}X^2 + 2Xx\cos(\omega t) + x^2\cos^2(\omega t) + 2(X + x\cos(\omega t)) \\ e^{-X}[I_0(x) - 2I_1(x)\cos(\omega t) + 2I_2(x)\cos(2\omega t) - 2I_3(x)\cos(3\omega t)] \\ +e^{-2X}[I_0(2x) - 2I_1(2x)\cos(\omega t) + 2I_2(2x)\cos(2\omega t) - 2I_3(2x)\cos(3\omega t)]\end{matrix}\right\} \tag{18}$$

Identifies the harmonics produced by V_{GS} modulation, without considering the saturation term. In contrast, I_D does consider V_{DS} modulation,

$$I_D = I_{ref}\left\{\begin{matrix}-e^{Y}[I_0(2x) + 2I_1(2x)\cos(\omega t) + 2I_2(2x)\cos(2\omega t) + 2I_3(2x)\cos(3\omega t)] \\ \times [I_0(y) - 2I_1(y)\cos(\Omega t) + 2I_2(y)\cos(2\Omega t) - 2I_3(y)\cos(3\Omega t)]\end{matrix}\right\} \tag{19}$$

Once V_{DS} modulation is considered, harmonics arise, and if analyzed in more detail, these harmonics can be grouped into four different categories:

$$\begin{aligned}I_{out} &= I_{ref}(A_0 + A_1\cos(\omega t) + A_2\cos(2\omega t) + A_3\cos(3\omega t)) + \\ &I_{ref}(B_0 + B_1\cos(\omega t) + B_2\cos(2\omega t) + B_3\cos(3\omega t)) + \\ &I_{ref}(D_1\cos(\Omega t) + D_2\cos(2\Omega t) + D_3\cos(3\Omega t)) + I_{ref}(IMH_v)\end{aligned} \tag{20}$$

Then, the normalized variables introduced above with respect to the I_{ref} current are applied. Using Equations (18) and (19), they are substituted into Equation (17), and Equation (20) is rewritten.

$$\begin{aligned}I_{out} = I_{ref}&\left\{\begin{matrix}X^2 + 2Xx\cos(\omega t) + x^2\cos^2(\omega t) + 2(X + x\cos(\omega t)) \\ e^{-X}[I_0(x) - 2I_1(x)\cos(\omega t) + 2I_2(x)\cos(2\omega t) - 2I_3(x)\cos(3\omega t)] \\ +e^{-2X}[I_0(2x) - 2I_1(2x)\cos(\omega t) + 2I_2(2x)\cos(2\omega t) - 2I_3(2x)\cos(3\omega t)]\end{matrix}\right\} \\ +I_{ref}&\left\{\begin{matrix}-e^{Y}[I_0(x) + 2I_1(2x)\cos(\omega t) + 2I_2(2x)\cos(2\omega t) + 2I_3(2x)\cos(3\omega t)] \\ \times [I_0(y) - 2I_1(y)\cos(\Omega t) + 2I_2(y)\cos(2\Omega t) - 2I_3(y)\cos(3\Omega t)]\end{matrix}\right\}\end{aligned}$$

Arithmetic operations are performed on the expression obtained using algebraic properties (distributive, associative). Then, from the calculations performed, an expression is arrived at that includes the four groups of harmonics.

$$\begin{aligned}I_{out} &= I_{ref}\left[X^2 + \frac{x^2}{2} + 2XI_0(x)e^{-X} - 2xe^{-X}I_1(x) + e^{-2X}I_0(2x)\right] + \\ &I_{ref}[2Xx + 2xe^{-X}[I_0(x) + I_2(x)] - 4Xe^{-X}I_1(x) - 2e^{-2X}I_1(2x)]\cos(\omega t) + \\ &I_{ref}\left[\frac{x^2}{2} + 4Xe^{-X}I_2(x) - 2xe^{-X}[I_1(x) + I_3(x)] + 2e^{-2X}I_2(2x)\right]\cos(2\omega t) + \\ &I_{ref}[-4Xe^{-X}I_3(x) + 2xe^{-X}I_2(x) - 2e^{-2X}I_3(2x)]\cos(3\omega t) +\end{aligned}$$

$$I_{ref}\begin{Bmatrix}-e^{Y}[I_0(2x)I_0(y)]-e^{Y}[2I_1(2x)I_0(y)]\cos(\omega t)-e^{Y}[2I_2(2x)I_0(y)] \\ \cos(2\omega t)-e^{Y}[2I_3(2x)I_0(y)]\cos(3\omega t)+e^{Y}[2I_1(y)I_0(2x)]\cos(\Omega t) \\ -e^{Y}[2I_2(y)I_0(2x)]\cos(2\Omega t)+e^{Y}[2I_3(y)I_0(2x)]\cos(3\Omega t)- \\ e^{Y}[2I_1(2x)\cos(\omega t)+2I_2(2x)\cos(2\omega t)+2I_3(2x)\cos(3\omega t)]\times \\ [-2I_1(y)\cos(\Omega t)+2I_2(y)\cos(2\Omega t)-2I_3(y)\cos(3\Omega t)]\end{Bmatrix}$$

The contribution of V_{GS} modulation to the harmonic content can be described through the following normalized expressions:

$$A_0 = X^2+\frac{x^2}{2}+2XI_0(x)e^{-X}-2xe^{-X}I_1(x)+e^{-2X}I_0(2x) \quad (21)$$

$$A_1 = 2Xx+2xe^{-X}[I_0(x)+I_2(x)]-4Xe^{-X}I_1(x)-2e^{-2X}I_1(2x) \quad (22)$$

$$A_2 = \frac{x^2}{2}+4Xe^{-X}I_2(x)-2xe^{-X}[I_1(x)+I_3(x)]+2e^{-2X}I_2(2x) \quad (23)$$

$$A_3 = -4Xe^{-X}I_3(x)+2xe^{-X}I_2(x)-2e^{-2X}I_3(2x) \quad (24)$$

The subsequent set is associated with the normalized amplitudes.

$$B_0 = -e^{Y}[I_0(2x)I_0(y)];\ B_1 = -e^{Y}[2I_1(2x)I_0(y)];$$

$$B_2 = -e^{Y}[2I_2(2x)I_0(y)];\ B_3 = -e^{Y}[2I_3(2x)I_0(y)] \quad (25)$$

These harmonics only arise when there is modulation by both. V_{GS} and V_{DS}. In the saturation region, the following condition must be met: $nV_{DS0} > V_{GS0} - V_{TH}$. Therefore, an increase in V_{DS0} causes the harmonics to decrease. Now, if V_{DS0} is small, modulation by V_{GS} must be considered, so in Equation (25), $I_0(y) = 1$ must be established.

The third group of harmonics also arises when there is modulation of both. V_{GS} and V_{DS}. Its expression with normalized amplitudes is as follows:

$$D_1 = e^{Y}[2I_1(y)I_0(2x)];$$

$$D_2 = -e^{Y}[2I_2(y)I_0(2x)];\ D_3 = e^{Y}[2I_3(y)I_0(2x)] \quad (26)$$

When modulation is introduced through V_{DS}, relation (26) yields $I_0(2x) = 1$. The resulting components are particularly relevant under low drain bias operation and become increasingly attenuated at higher V_{DS} levels.

Finally, the last group of harmonics is that of intermodulation IMH_v, and its normalized expression is as follows.

$$IMH_v = \begin{Bmatrix}-e^{Y}[2I_1(2x)\cos(\omega t)+2I_2(2x)\cos(2\omega t)+2I_3(2x)\cos(3\omega t)] \\ \times[-2I_1(y)\cos(\Omega t)+2I_2(y)\cos(2\Omega t)-2I_3(y)\cos(3\Omega t)]\end{Bmatrix} \quad (27)$$

Both the experimental results in [9] and the analytical model in [13] suggest that $I_1(x)$ becomes dominant over $I_2(x)$ and $I_3(x)$ As x increases, which is consistent with the behavior described by (12). Therefore, the principal intermodulation terms derived from (27) are given by:

$$\begin{aligned} IMH &= -e^{Y}[2I_1(2x)\cos(\omega t)][-2I_1(y)\cos(\Omega t)] \\ &= 4e^{Y}I_1(2x)I_1(y)\cos(\Omega t)\cos(\omega t) \\ &= 4e^{Y}I_1(2x)I_1(y)\left(\frac{\cos((\Omega+\omega)t)+\cos((\Omega-\omega)t)}{2}\right) \\ &= 2e^{Y}I_1(2x)I_1(y)\cos((\Omega+\omega)t)+ \\ &\quad 2e^{Y}I_1(2x)I_1(y)\cos((\Omega-\omega)t)\end{aligned}$$

$$IMH_{\Omega+\omega} = 2e^{Y}I_1(2x)I_1(y)\cos((\Omega+\omega)t) \quad (28)$$

and

$$IMH_{\Omega-\omega} = 2e^{Y}I_1(2x)I_1(y)\cos((\Omega-\omega)t) \quad (29)$$

This expression, as explained above, shows the highest amplitude values.

Table 1 presents the additional intermodulation harmonic resulting from the trigonometric. This table excludes the exponential factor. e^{Y}as well as the sign of each term. If we recall that the normalized variable Y depends on V_{DS}, the multiplier suggests that increasing the value of V_{DS} can reduce the amplitude of these harmonics.

Table 1. Intermodulation harmonic coefficients

	$\boldsymbol{\cos\omega t}$	$\boldsymbol{\cos 2\omega t}$	$\boldsymbol{\cos 3\omega t}$
$\cos\Omega t$	$2I_1(2x)I_1(y)$	$2I_2(2x)I_1(y)$	$2I_3(2x)I_1(y)$
$\cos 2\Omega t$	$2I_1(2x)I_2(y)$	$2I_2(2x)I_2(y)$	$2I_3(2x)I_2(y)$
$\cos 3\Omega t$	$2I_1(2x)I_3(y)$	$2I_2(2x)I_3(y)$	$2I_3(2x)I_3(y)$

6. The Third and Second Harmonic and Polarization of the CS Stage

This section focuses on the harmonic analysis of a transistor fabricated using 65nm technology. Key parameters for this process include a threshold voltage. V_{TH} of $0.24V$, a transconductance factor μC_{ox} of $983\mu A/V^2$, which was derived by extrapolating data from reference [10], a substrate factor n of 1.3 was considered, together with a thermal voltage $\phi_t$of $25.9mV$. Simulations were carried out using a transistor with a width to length ratio W/L of $50\mu m$ to $0.36\mu m$.

$$I_{ref} = 2(\mu C_{ox})\frac{W}{L}n\phi_t^2 \approx 238\mu A$$

The normalization current is calculated to be $I_{ref} = 238\mu A$. The simulations presented here are based on a drain-source voltage V_{DS} of $1V$, which corresponds to the standard operating Voltage for this technology. Neglecting drain modulation effects allows the analysis to focus on the relationship between bias conditions and harmonic distortion. In low-power amplifier operation, the moderate inversion region becomes especially relevant for suppressing third-order nonlinear components. The behavior of the current third harmonic as a function of V_{GS0} is therefore evaluated. Equation (7), without the saturation component, represents the transition between moderate and strong inversion. The exponential contribution within the first parenthesis is dominant at lower inversion levels, while the algebraic contribution becomes dominant as inversion increases.

Figure 2 illustrates two superimposed curves: the logarithm of I_{DS} and its derivative relative to V_{GS}. The moderate inversion region is marked, clearly visible within the voltage range of V_{GS} between $0.3V$ and $1V$.

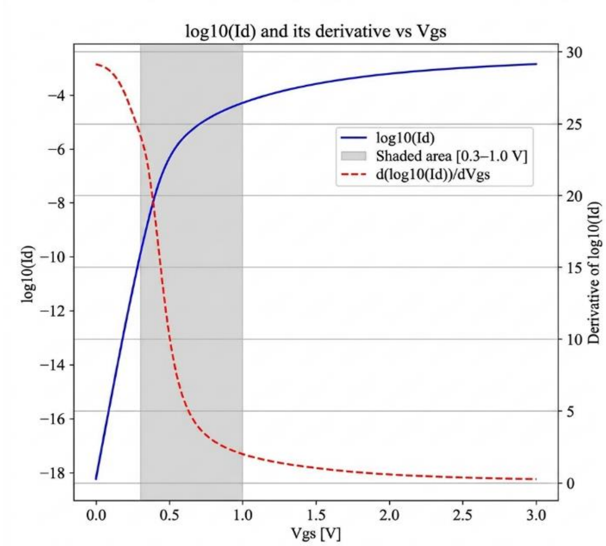

Fig. 2 Logarithmic drain current (I_{DS}) and its derivate with respect to V_{GS}

In the transition, neither the exponential term nor the algebraic term dominates completely; rather, both contribute in a similar way.

$$e^{-\frac{V_{GS}-V_{TH}}{2n\phi_t}} = \frac{V_{GS}-V_{TH}}{2n\phi_t}$$

To simplify, a definition is established.

$$X = \frac{V_{GS}-V_{TH}}{2n\phi_t}$$

So, the equation becomes,

$$e^{-X} = X$$

The transition between operating is characterized by the Voltage. V_{GST}, which is given by the following relation:

$$e^{-X} = X \tag{30}$$

To estimate the root of $f(X) = e^{-X} - X$, an iterative procedure based on the Newton-Raphson method, is employed.

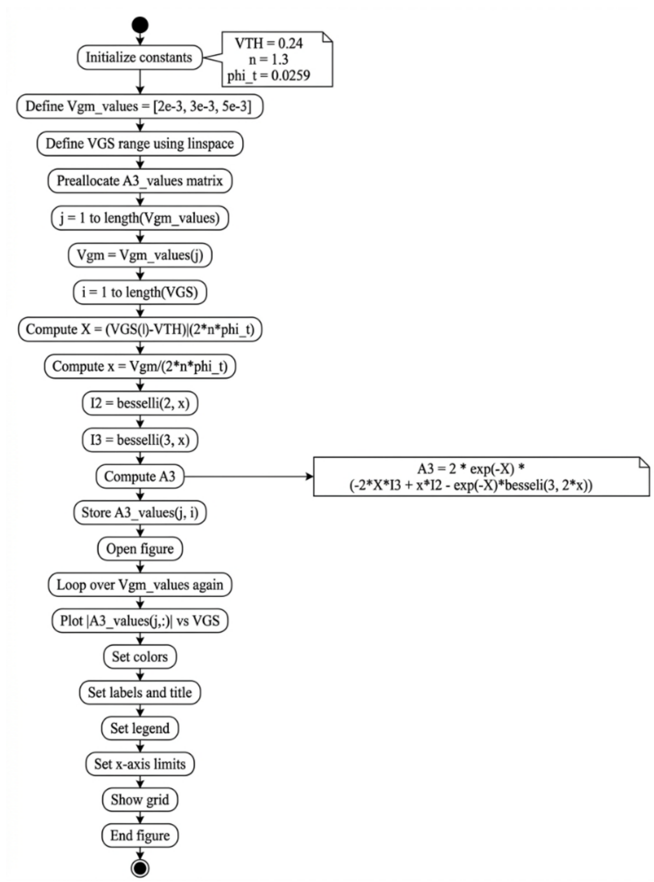

Fig. 3 MATLAB implementation flowchart for third harmonic calculation.

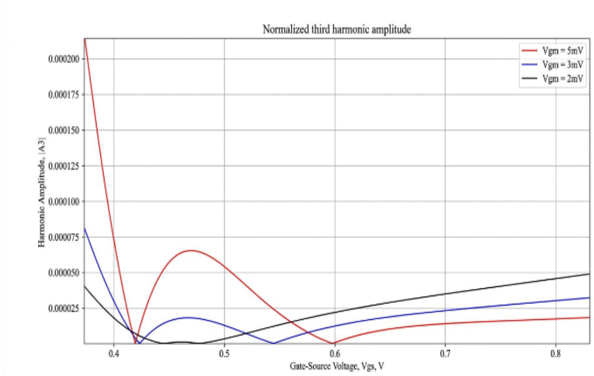

Fig. 4 Normalized third harmonic amplitude.

By applying the numerical procedure, convergence is achieved after at least three iterations. The resulting root is $X = 0.567$. Based on this result, the following expression is obtained:

$$X = \frac{V_{GS} - V_{TH}}{2n\phi_t}$$

When substituting the root obtained, the value of V_{GST} is:

$$0.567 = \frac{V_{GST} - 0.24}{2 \times 1.3 \times 25.9 \times 10^{-3}} \Rightarrow V_{GST} = 0.278V$$

Approximately $0.3V$. Therefore, V_{GST} marks the practical transition between the moderate inversion and strong inversion regions. Now, let us revisit Equation (24) and express it in the following form:

$$A_3 = 2e^{-X}[-2XI_3(x) + xI_2(x) - e^{-X}I_3(2x)] \quad (31)$$

By evaluating $|A_3|$ (Figure 4) and using the corresponding process parameters, two bias points are identified at which this harmonic component vanishes. Identifying these values requires solving the nonlinear equation.

$$2e^{-X}[-2XI_3(x) + xI_2(x) - e^{-X}I_3(2x)] = 0$$

$$-2XI_3(x) + xI_2(x) - e^{-X}I_3(2x) = 0 \quad (32)$$

The MATLAB implementation for the third harmonic calculation is summarized in Figure 3.

The Equation (32) depends on two parameters, where X represents the bias value and x is the signal amplitude. To separate the equation into two terms, one depending on the bias and the other on the signal amplitude, the approximations described in Equation (12) can be substituted. This yields the following result.

$$A_3 = \frac{x^3 e^{-X}}{12}(-X + 3 - 4e^{-X}) = x^3 F_3(X) \quad (33)$$

The term $F_3(X)$ is known as the third-order harmonic distortion factor. Therefore, bias points corresponding to the zeros of this function result in a null third harmonic amplitude.

$$-X + 3 - 4e^{-X} = 0 \quad (34)$$

The analysis of the equation shows that it reaches a local maximum at $X = ln(4)$, which indicates that at this point the function stops growing and begins to decrease. Similarly, the Newton-Raphson numerical method will be used to find the roots.

The first root is between 0 and 1, whereas the second root is between 2 and 3. Convergence is achieved after four iterations, yielding approximate solutions $X_1 \approx 0.450$ and $X_2 \approx 2.742$.

Which leads to a gate source voltage of $V_{GS1} = 0.270V$ and $V_{GS2} = 0.425V$, respectively. The first solution corresponds to a bias condition within the moderate inversion region. The appropriateness of this operating point for low-distortion amplification is assessed by verifying that the chosen bias voltage. $V_{GS0} = 0.270V$ remains above the threshold voltage V_{TH}.

$$V_{TH} = 0.24V, V_{GS0} = 0.270V \rightarrow V_{GS0} > V_{TH}$$

Achieving this condition would demand a threshold. V_{TH} tolerance of around 10%, which is not practical in real implementations.

$$0.216V < V_{TH} < 0.264V$$

Figure 6 shows how the magnitude of $|F_3|$ varies within the V_{TH} tolerance range for a fixed V_{GS0}.

Therefore, with a tolerance of 10%, V_{TH} lies between 0.216V and 0.264V. For $V_{TH} = 0.24V$ and $V_{GS0} = 0.270V$, the amplitude $|F_3|$ becomes zero.

As V_{TH} tends to 0.263V, the amplitude of $|F_3(X)|$ starts to grow. When it gets closer to 0.268V, the growth is more noticeable, which means that third order harmonic distortion is getting worse.

$$|F_3(X)| \approx 0.05325$$

For an amplitude modulation signal where V_{GM} equals 2 mV.

- When allowing a 10% variation in the threshold voltage V_{TH}, distortion remains nearly insignificant. However, achieving this level of precision is unrealistic given the tight manufacturing tolerances needed.
- With a more feasible tolerance of 50%, the third-order harmonic distortion rises sharply, surpassing the maximum allowable value of $|F_3|_{max} = 0.0162$.
- Even by tuning the gate-source voltage V_{GS} to its optimal points, the harmonic distortion continues to exceed acceptable levels throughout the entire tolerance range.

In summary, for a modulation voltage $V_{GM} = 2mV$, third-order distortion cannot be avoided when considering realistic variations in the threshold voltage V_{TH}. Eliminating this distortion would demand a tolerance tighter than 10%, a level of precision that is impractical for both design and manufacturing processes.

For a modulation signal where $V_{GM} = 3mV$, the following observations are made:

- At a gate-source voltage $V_{GS} = 0.4229V$ with a 10% tolerance, harmonic distortion is minimized near $V_{TH} = 0.24V$, though the acceptable tolerance window is quite limited.
- Increasing V_{GS} to 0.468V allows for a broader tolerance of up to 25% without surpassing the harmonic distortion threshold.
- When the tolerance expands to 50%, issues arise again; harmonics are suppressed to the left of V_{TH}, but they rise steeply on the right side.
- By further adjusting V_{GS} to 0.541V, harmonic distortion remains within acceptable limits even at 50% tolerance, offering a practical engineering solution.
- Although higher V_{GS} values, like 0.577V, also control harmonic levels; they lead to excessive linearity, potentially reducing system sensitivity and impairing dynamic performance.

When $V_{GM} = 3mV$, the ideal operating point occurs at $V_{GS} = 0.541V$. This setting accommodates a practical tolerance of up to 50% in V_{TH} without surpassing distortion limits, successfully balancing distortion levels and linearity. The MATLAB implementation for the third harmonic distortion factor calculation is summarized in Figure 5.

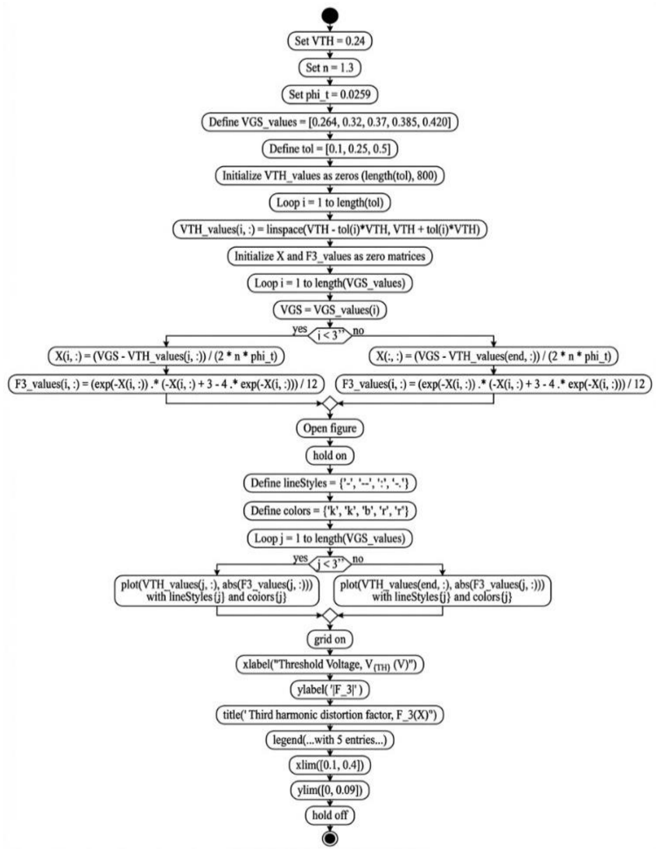

Fig. 5 MATLAB implementation flowchart for third harmonic distortion factor calculation

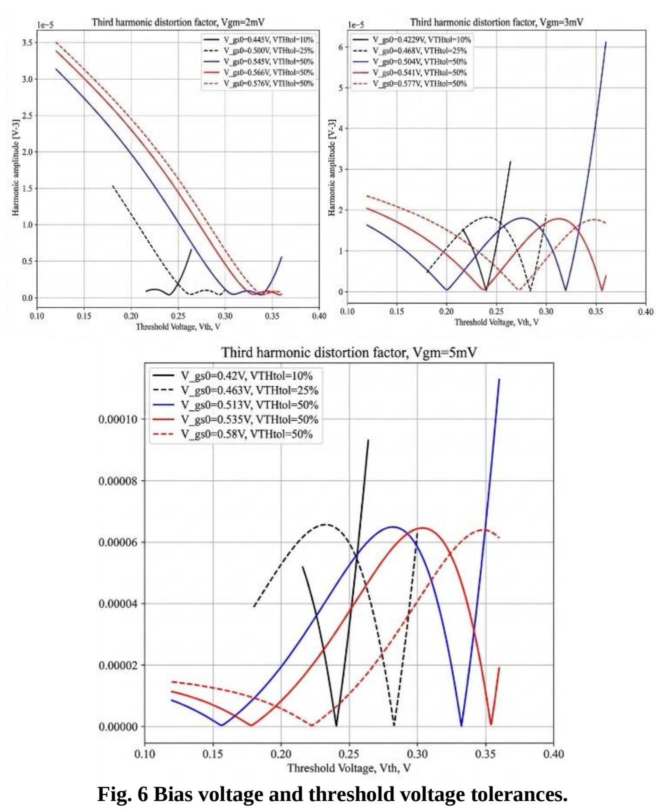

Fig. 6 Bias voltage and threshold voltage tolerances.

For $V_{GM} = 5mV$, similar trends to those seen at $V_{GM} = 3mV$ are evident, but with important distinctions:

- The higher V_{GM} value intensifies the amplitude of the curves, spreading out the null points, or "sweet spots," which complicates precise management of the harmonic cancellation region.
- At $V_{GS} = 0.42V$, harmonics are canceled near $V_{TH} = 0.24V$ within a 10% tolerance, though slight deviations cause a rapid rise in harmonic distortion.
- Increasing V_{GS} to 0.463V allows for a 25% tolerance without the harmonics exceeding acceptable limits; however, the effective operating range remains narrow.
- With a 50% tolerance at $V_{GS} = 0.513V$, two cancellation points appear, but surpassing the second "sweet spot" results in a steep increase in harmonics.
- Finally, setting V_{GS} to 0.58V keeps harmonic distortion within permissible bounds, yet it introduces a zone of excessive linearity, which could trigger instability and other adverse effects.

The best operating point occurs at $V_{GS} = 0.535V$, where a 50% tolerance in V_{TH} enables the achievement of two cancellation points without causing sudden spikes in distortion or excessive linearity. It is important to make comparisons between different. V_{GS} values, as this allows the tolerance value for V_{TH} to be analyzed. For a V_{GS0} A value of 0.320V, a tolerance of 25% is required V_{TH}.

This means that V_{TH} is within the range of 0.18V to 0.30V. In this range,$|F_3|$ attains a peak value of 0.0162 between X_1 and X_2.

If we now consider an even higher tolerance 50%, which is a little more realistic,

$$0.12V < V_{TH} < 0.36V$$

The threshold voltage lies in the range 0.12V to 0.36V. At $V_{GS0} = 0.37V$, conditions favor $|F_3|$ values surpassing $|F_3|_{max}$ for devices characterized by elevated V_{TH}, as depicted in Figure 6.

A certain value of $V_{GS0} = 0.385V$ is attained by raising the bias voltage (Figure 6 red line). This value ensures that $|F_3|$ remains below the maximum distortion value, $|F_3|_{max} = 0.0162$, across the entire V_{TH} range. Therefore, the graph serves as a reference for designing amplifiers with low distortion. It is therefore advisable to rely on the distortion factor value for designs. Increasing the value of V_{GS0} causes $|F_3|$ to decrease. However, this results in greater power dissipation by the transistor and less favorable performance.

Now, let's consider the term B_3 that contributes to the third harmonic (eq. 25). If there is no modulation by V_{DS}, the value of $I_0(y) = 1$ must be considered. Therefore, by applying the approximation for $I_3(2x)$ as given in Equation (12),

$$B_3 = -e^Y[2I_3(2x)I_0(y)]$$

It is obtained

$$B_3 = -e^Y(x^3/3) \quad (35)$$

If it becomes necessary to diminish B_3 in relation to A_3, A suppression coefficient can be introduced and defined accordingly.

$$S_{3dg} = \frac{|B_3|}{|A_3|} \quad (36)$$

Therefore, from the analysis of (33) and (35), the required source-drain voltage V_{DS0} is obtained as:

$$|x^3F_3(X)|S_{3dg} = \left|\frac{-e^Y x^3}{3}\right|$$

$$e^Y = 3|F_3(X)|_{max}S_{3dg} \quad (37)$$

Recall that Y is defined as $Y = \frac{V_{GS0} - V_{TH} - nV_{DS0}}{n\phi_t}$. Accuracy requires the use of the minimum. V_{TH} in the evaluation process.

$$\ln(e^Y) = \ln\left(3|F_3(X)|_{\max} S_{3dg}\right)$$
$$Y = \ln\left(3|F_3(X)|_{\max} S_{3dg}\right)$$

$$Y = \frac{V_{GS0} - V_{TH} - nV_{DS0}}{n\phi_t} = \ln\left(3|F_3(X)|_{\max} S_{3dg}\right) \quad (38)$$

As an illustration, for $V_{GS0} = 0.385V$, the threshold voltage is adjusted to its minimum value, $V_{TH} = V_{THmin} = 0.120V$.

This is the lowest threshold value that allows for a 50% tolerance margin. Under these conditions, achieving a drain current sensitivity S_{3dg} of 0.01, requires V_{DS}=0.257 V. Using the values provided, Equation (38) will yield the following value for V_{DS}. For the values $V_{GS} = 0.385V$ and $V_{TH} = 0.120V$, the difference is $V_{GS} - V_{TH} = 0.265V$. Consequently, the value of $V_{DS} = 0.257V$ mentioned is slightly below the saturation threshold.

$$V_{DS0} = \frac{V_{GS0} - V_{TH}}{n} - \phi_t ln\left(3|F_3|_{max}S_{3dg}\right)$$

$$V_{DS0} = \frac{0.385 - 0.120}{1.3} - (0.0259)ln\left(3(0.0162)(0.01)\right)$$

$$V_{DS0} = 0.4014$$

For $V_{DS} = 0.257V$, it would be necessary to modify values such as V_{TH} or V_{GS}. This is because with the values mentioned, a $V_{DS} = 0.401V$ is obtained. The difference $(0.385 - 0.260)V$, which is equivalent to 0.125V, shows that the value of $V_{TH} = 0.260V$, which ensures that we are in the saturation region ($nV_{DS} > |V_{GS} - V_{TH}$). Using this result, the corresponding V_{DS} is 0.294V. What must always be achieved is that V_{DS} is greater than that difference. With this, it can be verified that it is in the saturation region.

$$V_{DS0} = \frac{0.385-0.260}{1.3} - (0.0259)ln\big(3(0.0162)(0.01)\big)$$

$$V_{DS0} = 0.2938V$$

The same analytical procedure used for the third harmonic is applied to obtain the second harmonic component. Equation (23) can then be expressed as:

$$A_2 = \frac{x^2}{2} + 4Xe^{-X}I_2(x) - 2xe^{-X}[I_1(x) + I_3(x)] + 2e^{-2X}I_2(2x)$$

$$A_2 = \frac{x^2}{2} + 2e^{-X}\{2XI_2(x) - x[I_1(x) + I_3(x)] + e^{-X}I_2(2x)\} \quad (39)$$

The dependence of A_2 on V_{GS} is presented in Figure 7 under different excitation amplitudes V_{gm}. Then, from Equation (39), we can obtain the V_{GS} value that minimizes A_2. To do this, we will use Eq. (12) to reduce and obtain the following:

$$A_2 = \frac{x^2}{2}\left[1 + e^{-X}\left(X - 2 - \frac{x^2}{3} + 2e^{-X}\right)\right]$$

$$A_2 = x^2 F_2(x, X) \quad (40)$$

Analyzing these values, $F_2(X, x)$ hardly changes, and therefore we can state that:

$$F_2(x, X) \approx F_2(X) = \frac{1}{2}\{1 + e^{-X}(X - 2 + 2e^{-X})\}$$

$$F_2(X) = \frac{1}{2}\{1 + e^{-X}\big(X - 2(1 - e^{-X})\big)\} \quad (41)$$

To solution to the equation $F_2(X) = 0$, is obtained by analyzing the following

$$0.5e^{-X}\,(-X + 3 - 4e^{-X}) = 0$$

Noting that the equation shares the same structure as (34), its solutions can be directly identified, $X \approx 0.450$ ($V_{GS0} = 0.2703V$) and $X \approx 2.742$ ($V_{GS0} = 0.4246V$). Evaluate the roots obtained in $F_2(X)$. The function $F_2(X)$ reaches a minimum value of 0.412, at $X = 0.450(V_{GS0} = 0.270V)$ and a flat maximum of 0.528 at $X = 2.742(\ V_{GS0} = 0.420\ V)$. Using a 65nm MOSFET transistor model, simulations performed in NGSpice have confirmed the harmonic response of the device in a series of bias scenarios.The above result shows that. $F_2(X)$ reaches a flat peak for $V_{GS0} = 0.420\ V$. When the simulation is run at real frequencies, more details of its behavior can be seen. When considering a fundamental frequency of 2 kHz, multiple harmonics can be observed for V_{GS} values below 0.6 V. Now, if V_{GS} tends towards 0.6V, the MOSFET enters the saturation region, which means that the simulation results show that the second harmonic disappears almost completely. With V_{GS} values greater than 0.6V, the response of the second harmonic of the MOSFET exhibits almost linear behavior. This remains constant, which coincides with the theoretical results obtained. Therefore, second-order distortion remains essentially constant within the operating range. This behavior is observed for all tested. V_{GM} values ($2mV, 4mV, 6mV$, and $8mV$), with only minor variations in the signal. While second harmonic distortion is reduced, third harmonic distortion still persists even within the saturation region. This observation is consistent with theoretical findings, which highlight that the main objective is usually to minimize the $|A_3|$ component, given its resistance to elimination by standard design methods or filtering approaches.

The MATLAB implementation for the second harmonic calculation is summarized in Figure 8.

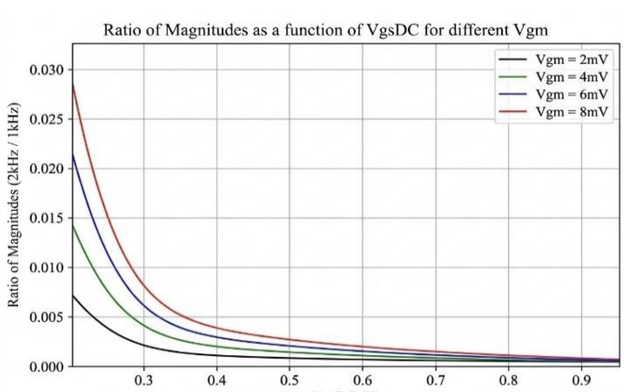

Fig. 7 Behavior of the normalized second harmonic under different bias voltage conditions

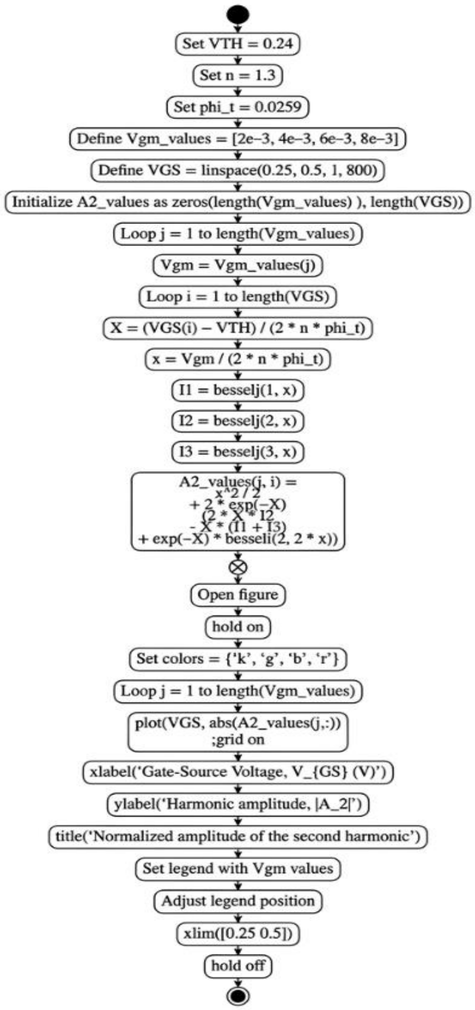

Fig. 8 MATLAB implementation flowchart for second harmonic calculation

Generally, the key aim is to reduce the magnitude of the third harmonic $|A_3|$ while also minimizing power consumption. When considering the potential reduction of A_2, It is essential to relate this to the tolerance levels of V_{TH}, as discussed earlier. According to Figure 9, obtained. $F_{2min}(X) = 0.412$ demands tight control of the V_{TH} tolerance, often limited to less than 10%. However, this improvement is limited to roughly a 20% gain compared to a tolerance of 50%. The key takeaway is that. $F_{2max}(X) = 0.528$ remains almost unaffected by bias variations within the critical range for minimizing $|A_3|$. The term B_2, which contributes to the second harmonic, is defined by Equation (25). In scenarios without drain voltage modulation, $I_0(y)$ should be treated as 1 when calculating B_2. Therefore, the approximations in Eq. (12) can be applied to $I_2(2x)$, yields the following:

$$B_2 = -e^{Y} x^2 \tag{42}$$

The MATLAB implementation for the second harmonic distortion factor calculation is summarized in Figure 10.

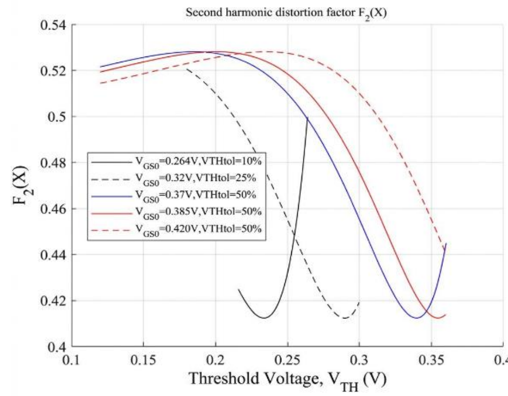

Fig. 9 Sensitivity of circuit performance to variations in bias voltage and threshold voltage.

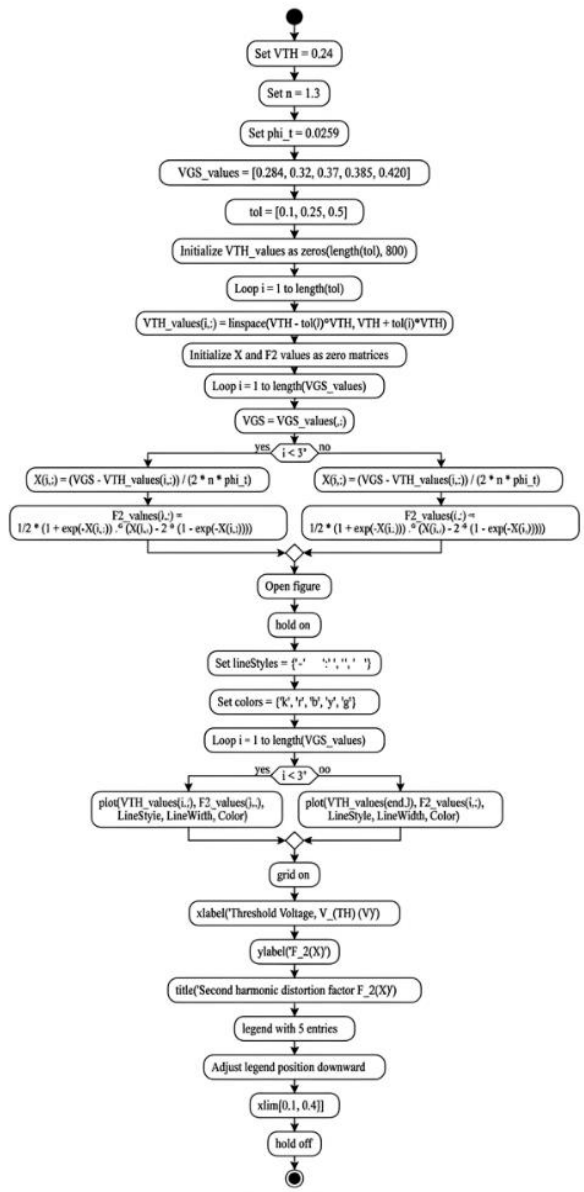

Fig. 10 MATLAB implementation flowchart for second harmonic distortion factor calculation

To quantify the attenuation effect, a suppression factor is introduced.

$$S_{2dg} = \frac{|B_2|}{|A_2|} \tag{43}$$

If the bias condition V_{GS0} is determined from third-order distortion requirements, the approximation $A_2 \approx x^2 F_{2max}$ becomes valid, from which S_{2dg} can be evaluated:

$$S_{2dg} = \frac{|-x^2 e^Y|}{|x^2 F_2(X)|} = \frac{e^Y}{F_2(X)}$$

$$S_{2dg} = \frac{e^Y}{F_{2max}} \tag{44}$$

Equation (44), together with $Y = (V_{GS0} - V_{TH} - nV_{DS0})\ /n\phi_t$, allows expressing the bias voltage V_{DS0} as:

$$\ln\left(e^Y\right) = \ln\left(S_{2dg} F_{2\max}(X)\right)$$

$$Y = \frac{V_{GS0} - V_{TH} - nV_{DS0}}{n\phi_t} = \ln\left(S_{2dg} F_{2\max}(X)\right) \tag{45}$$

For the calculation, V_{TH} should be considered to be 0.120V, remembering that this is the minimum value when 50% tolerance was considered. With this value, more accurate results will be obtained. The preceding analysis provides the basis for defining a procedure to select the gate to source voltage for low distortion operation, as detailed below. Designers should be aware that obtaining the best points for the third and second harmonics requires very precise control of the threshold voltage, V_{TH}. An alternative approach is to select a bias voltage within the "sweet spots" identified in Figure 4, where $|F_3(X)|$ reaches its maximum. The bias condition is deemed acceptable when the associated third harmonic level and power dissipation are maintained below allowable thresholds. The threshold voltage represents one of the key design parameters. Its allowable variation is determined from the interval extending between $V_{TH_{max}}$ and $V_{TH_{min}}$, centered around the nominal value V_{TH}. These values are often difficult to determine accurately.

Therefore, the value of X will be found considering the nominal threshold voltage.

$$F_3(X) = \frac{[e^{-X}(-X+3-4e^{-X})]}{12} = 0.0162 \tag{46}$$

To solve the equation $e^{-X}(-X + 3 - 4e^{-X})/12 - 0.00162 = 0$, we first observe how the function corresponding to this equation $f(X) = e^{-X}(-X + 3 - 4e^{-X})/12 - 0.00162$ behaves. This nonlinear equation has two roots: $X_1 = 0.9713$ and X_2 = 3.8255.

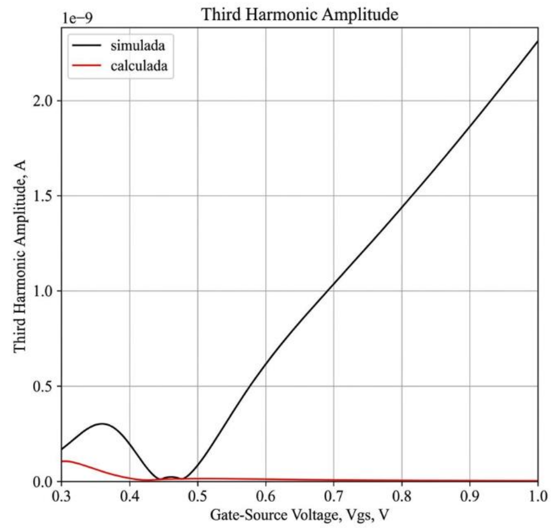

Fig. 11 Behavior of the normalized second harmonic under varying bias voltage conditions

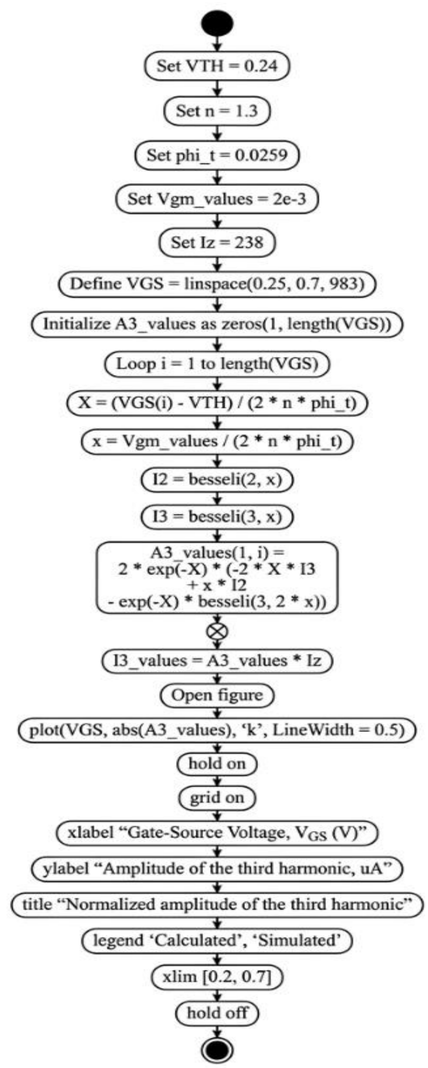

Fig. 12 MATLAB implementation flowchart for normalized amplitude of the third harmonic calculation

The MATLAB implementation for the normalized amplitude of the third harmonic calculation is summarized in Figure 12.

$$F_3(X_1) = \frac{[e^{-0.9713}(-0.9713+3-4e^{-0.9713})]}{12} = 0.0162$$

$$V_{GS} = 2n\phi_t X + V_{TH}$$

The bias voltage is:

$$V_{GS} = 2(1.3)(0.0259)(0.9713) + 0.24 = 0.3054V$$

Solving the equation results in $X = 0.971$, which corresponds to a bias voltage of approximately. $V_{GS} \approx 0.31V$ (with $V_{TH} = 0.24V, n = 1.3$, and $\phi_t = 25.9mV$).

This operating condition is subsequently analyzed through simulation using a transistor sized according to Y. Tsividis's model and capable of delivering the required current. Figure 11 illustrates the corresponding response.

The actual current values are recovered from the normalized quantities in Figure 4 through multiplication by 238 μA. The voltage drop across a 1Ω series resistor connected to the drain terminal was used to obtain the simulation results.

Then, these numbers were compared to theoretical predictions, with the assumption that the excitation voltage. $V_{GS} = 2\ mV$. A close correspondence is observed between the simulated "sweet" point and the theoretical value.

The peak happens around. $V_{GS} = 0.36V$, which is rather close to the calculated $V_{GS} = 0.31V$. Although a second "sweet" point exists at much higher gate source voltages, it is less significant. It is evident that the gate source voltage should be set near $V_{GS} = 0.35V$. Additional reduction of the third harmonic is achieved by shifting V_{GS} towards the second "sweet" point.

This corresponds to bias voltages approximately equal to or greater than 0.42V, with the tradeoff of increased power dissipation. The precise value of the threshold voltage tolerance (V_{TH}) is generally indeterminate, however it is well recognized that this parameter is contingent upon the channel length. To see how these changes effect performance, both the width and length of the transistor can be made smaller at the same time. This lets us see how these changes affect electrical properties.

This change doesn't affect the parameter. I_Z, hence the estimated characteristic stays the same. Scaling the transistor geometry to one-half of its initial dimensions leads to a considerable modification of the simulated behavior. Under this condition, the first "sweet" point appears near 0.31V, and the peak shifts to approximately 0.42V (Figure 13). This simulation again highlights that biasing solely at the "sweet" point is not recommended.

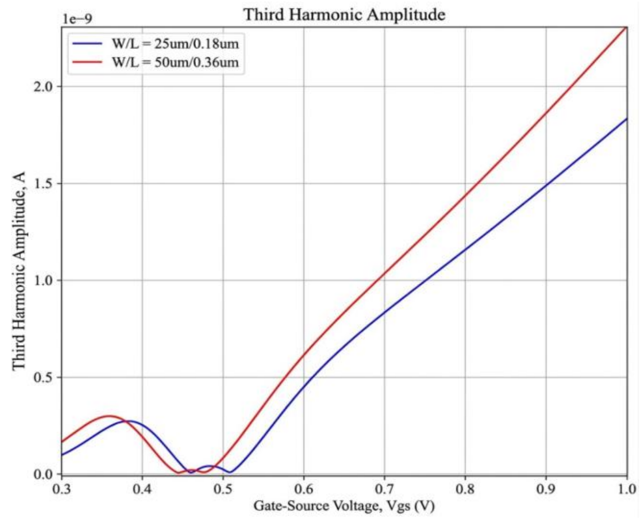

Fig. 13 BSIM4: Effect of transistor length on the third order harmonic amplitude for $V_{gm} = 2mV$

After selecting a bias level of 0.42V, it becomes essential to verify that the operating point stays stable despite variations in drain voltage, temperature changes, or assessments under different manufacturing process conditions.

If the criteria for minimizing harmonic distortions associated with the saturation region are satisfied, then the drain-source bias voltage should be fine-tuned, typically by increasing it. These steps generally summarize the key guidelines for designing a common-source amplifier stage.

7. Intermodulation

This section presents simulation dependencies derived for non-standard drain-source voltages. V_{DS} below 1V. Raising the Voltage within this range effectively minimized fluctuations in the saturation part of the model.

Figure 1 demonstrates how drain modulation impacts the computation of these components. By applying the approximations from Equation (12) following the formulation in [13], assuming y is not zero, and the modulation signal has an amplitude similar to the input signal x, it follows that:

$$B_2 = -e^Y[2I_2(2x)I_0(y)] = -e^Y\left[2\left(\frac{4x^2}{8}\right)\left(1+\frac{y^2}{4}\right)\right]$$

$$|B_2| \approx e^Y x^2$$

$$D_2 = -e^Y[2I_2(y)I_0(2x)] = -e^Y\left[2\left(\frac{y^2}{8}\right)\left(1+\frac{4x^2}{4}\right)\right]$$

$$|D_2| \approx e^Y(y^2/4)$$

$$|B_2| \approx e^Y x^2; |D_2| \approx e^Y (y^2/4) \tag{47}$$

This leads to the following expression for the overall second harmonic amplitude.

$$|B_2| + |D_2| = e^Y x^2 + e^Y (y^2/4) \approx e^Y x^2 \left(1 + \frac{y^2}{4x^2}\right)$$
$$= e^Y x^2 \left(1 + \frac{\left(\frac{|y|}{|x|}\right)^2}{4}\right) \approx e^Y x^2 \left(1 + \frac{K_{dg}^2}{4}\right)$$

$$|B_2| + |D_2| \approx e^Y x^2 \left(1 + \frac{K_{dg}^2}{4}\right) \tag{48}$$

In this context, K_{dg} represents the ratio between the magnitudes of y and x. By following a similar approach, it can also be demonstrated that.

$$B_3 = -e^Y[2I_3(2x)I_0(y)] = -e^Y\left[2\left(\frac{8x^3}{48}\right)\left(1 + \frac{y^2}{4}\right)\right]$$
$$|B_3| \approx e^Y(x^3/3)$$
$$D_3 = e^Y[2I_3(y)I_0(2x)] = e^Y\left[2\left(\frac{y^3}{48}\right)\left(1 + \frac{4x^2}{4}\right)\right]$$
$$|D_3| \approx e^Y(y^3/24)$$
$$|B_3| \approx e^Y\left(\frac{x^3}{3}\right); |D_3| \approx e^Y\left(\frac{y^3}{24}\right) \tag{49}$$

The magnitude of the third harmonic component is expressed as:

$$|B_3| + |D_3| = e^Y\left(\frac{x^3}{3}\right) + e^Y\left(\frac{y^3}{24}\right) = e^Y \frac{x^3}{3}\left(1 + \frac{y^3}{8x^3}\right)$$
$$= e^Y \frac{x^3}{3}\left(1 + \frac{\left(\frac{|y|}{|x|}\right)^3}{8}\right) \approx e^Y \frac{x^3}{3}\left(1 + \frac{K_{dg}^3}{8}\right)$$

$$|B_3| + |D_3| \approx e^Y \frac{x^3}{3}\left(1 + \frac{K_{dg}^3}{8}\right) \tag{50}$$

It is evident that when the modulating signal is strong, the effects of drain modulation can be mitigated by increasing the suppression factors. S_{2dg} and S_{3dg}, which is achieved by operating at higher values of V_{DS}.

Table 2. Intermodulation coefficients obtained from the proposed analysis.

	$\cos(\omega t)$	$\cos(2\omega t)$	$\cos(3\omega t)$
$\cos(\Omega t)$	xy	$(x^2y)/2$	$(x^3y)/6$
$\cos(2\Omega t)$	$(xy^2)/4$	$(x^2y^2)/8$	$(x^3y^2)/24$
$\cos(3\Omega t)$	$(xy^3)/24$	$(x^2y^3)/48$	$(x^3y^3)/144$

The reduction of intermodulation harmonics follows a comparable approach. Table 2 displays the intermodulation coefficient values derived by applying the approximations from Equation (12) to the inputs listed in Table 1. The approximations make it possible to identify the leading intermodulation component, which, under specific input and drain modulation conditions, occupies the upper left portion of the table. When suppression criteria are set, such as limits on gate-source modulation, the required increase in drain-source voltage can be calculated using the same methodology applied to counteract drain modulation.

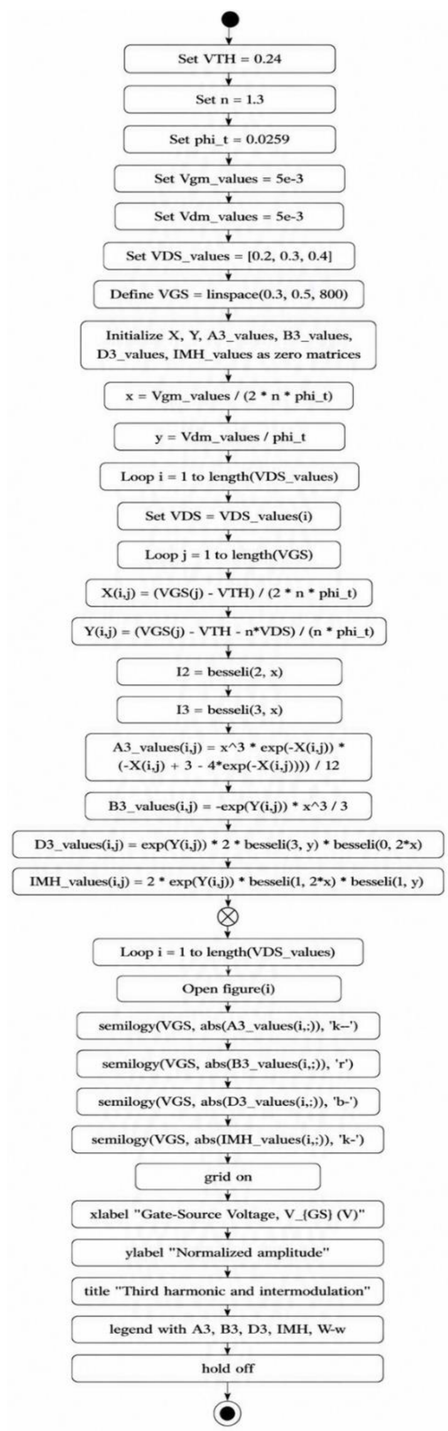

Fig. 14 MATLAB implementation flowchart for third harmonic and intermodulation calculation

According to Equation (25), the harmonic A_3 remains unaffected by the drain-source voltage V_{DS}. In contrast, the harmonics B_3, D_3, and all intermodulation harmonics exhibit a strong dependence on this Voltage. Figure 15 compares the behavior of the different components, including $IMH_{\Omega-\omega}$, B_3, D_3, and A_3, each represented with a distinct line style. All quantities were obtained in normalized form, considering gate and drain modulation voltages of 5mV.

We focus on the interval between 0.32 V and 0.40 V for V_{GS}, as this range is ideal for achieving low distortion in an amplifier. Figure 15(a) depicts results calculated at a drain-source voltage. V_{DS} of 0.2V. For V_{TH} of 0.24V and n of 1.3, the transistor operates in saturation. However, at this voltage level, intermodulation distortion is prominently high it can reach amplitudes nearly ten times greater than $|A_3|$. Moreover, the harmonics B_3 and D_3 may also exhibit amplitudes exceeding that of A_3.

This indicates that even without drain-source modulation, these components significantly affect the choice of V_{DS}. To lower the intermodulation harmonic to match the amplitude of A_3, the drain-source voltage must be raised to 0.3V, as illustrated in Figure 15(b). It is only when V_{DS} is further increased to 0.4V (see Figure 15(c), so that the intermodulation harmonic drops below A_3, making it reasonable to disregard the B_3 and D_3 components.

The MATLAB implementation for third harmonic and intermodulation calculation is summarized in Figure 14.

The graphs shown in Figure 15 can also be understood from another perspective. At elevated V_{DS} levels, the third harmonic component B_3 and D_3, together with the intermodulation current $IMH_{\Omega-\omega}$, are effectively diminished. In contrast, the third harmonic A_3 remains unaffected by changes in this Voltage. Next, we will analyze the simulation outcomes for a particular gate-source voltage scenario.

Table 3 displays the simulation results for a transistor with dimensions of $50\mu m$ by $0.36\mu m$, tested at a V_{GS} of 0.35V. The modulation signals used were $V_{gs} = 5mV$ at a frequency of 100MHz and $V_{ds} = 5mV$ at 110MHz.

It is evident that at $V_{DS} = 0.3V$, the third harmonic closely matches $I_3 = I_{ref}\, A_3 = 1.6\, nA$. From Figure 11, the data point corresponding to $V_{GS} = 0.32V$ can be taken and scaled by a factor 2.5^3, yielding approximately 15.6. Beyond this point, the third harmonic gradually increases as the drain-source voltage rises.

Notably, the current I_{10MHz} surpasses I_3 at voltages below $0.3V$. Moreover, instead of continuing to decrease, I_{10MHz} stabilizes and approaches a final asymptotic value as V_{DS} nears 0.5V.

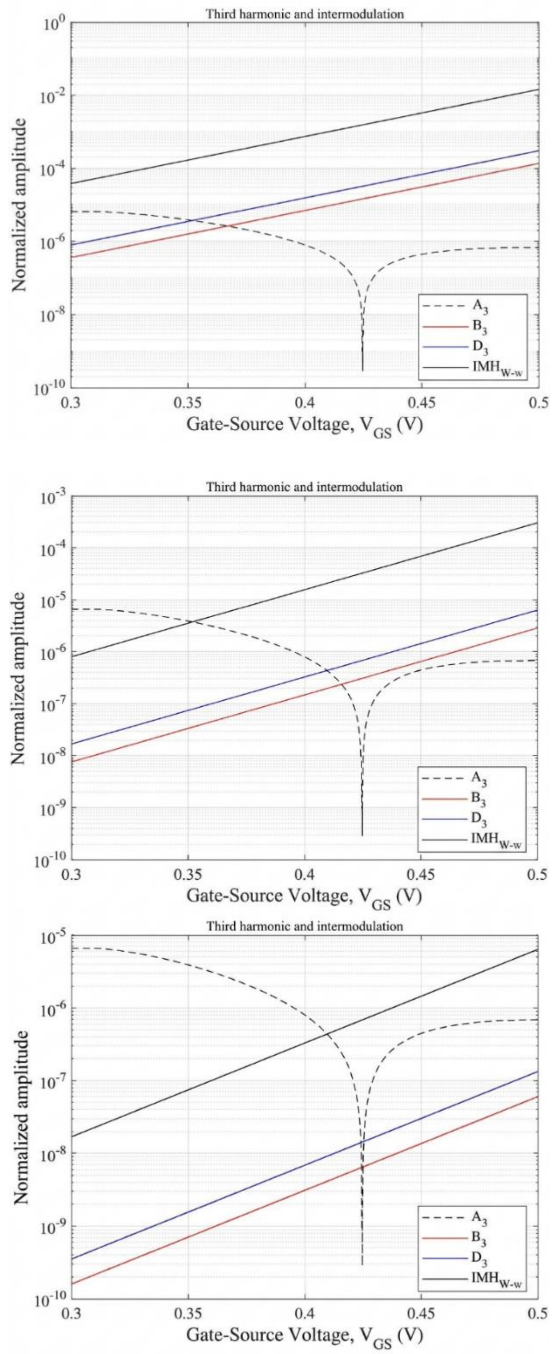

Fig. 15 Influence of third harmonic components on the intermodulation amplitude: $(a) V_{DS} = 0.2V, (b) V_{DS} = 0.3V, and\ (c)\ V_{DS} = 0.4V$

Table 3. Harmonic suppression

V_{DS}, V	0.2	0.3	0.4	0.5	0.6	0.7
I_3, nA	3.77	1.40	1.44	1.50	1.60	1.69
I_{10MHz}, nA	285	96.0	90.6	88.7	87.4	86.4

It cannot be guaranteed that this value exists at infinity with the model used. If you analyze the I_{10MHz} values in Table 3, you can see that the measured values are substantially higher than the values predicted by the model when V_{GS} is less than 0.3V. This disparity illustrates that the simple model does not accurately show how much intermodulation distortion there is, or the distortion that does not oscillate with the V_{DS} voltage. Therefore, a good technique to solve this problem is to include a multiplier that represents the modulation factor of the channel length, as suggested in [7].

Adding this factor to the harmonic distortion analysis would give us the term we need to model the persistent intermodulation distortion. This would make the derivation more complicated, but based on the result of this work, it is still doable and could be a good subject for future research.

8. Other Applications

8.1. 1dB Compression Point

The 1dB compression level can be obtained through harmonic analysis. Accordingly, the fundamental component associated with the drain current may be expressed as follows. The associated first-order harmonic component of the drain current is written as:

$$A_1 + B_1 = 2Xx - 4Xe^{-X} I_1(x) + 2xe^{-X}[I_0(x) + I_2(x)] \\ -2e^{-X} I_1(2x) - e^{Y}[2I_1(2x) I_0(y)] \quad (51)$$

Under negligible drain source modulation, $I_0(y)$ reduces to unity, and the bias parameter remains above one. In this context, 2X characterizes the linear amplification behavior. In this scenario, for $X > 1$, the term e^{-X} tends toward zero. By utilizing the approximations provided in Equation (12), it follows that.

$$A_1 + B_1 \approx 2Xx - e^{Y}[2I_1(2x)] = \left[2X - 2e^{Y}\left(1 + \frac{x^2}{2}\right)\right]x \quad (52)$$

The input signal that defines the 1dB compression point can be derived from the following equation:

$$Ef_{out} = \frac{CalculatedOut(includingnonlinearities)}{IdealLinearGain}$$

$$Ef_{out} = \frac{X - 2e^{Y}\left(1 + \frac{x^2}{2}\right)}{X}$$

Power gain expressed in decibels (dB)

$$G_{dB} = 10\, log\left(\frac{P_{out}}{P_{int}}()^{\frac{G_{dB}}{10}}\right)$$

Nevertheless, $P \propto A^2$

$$A = 10^{-\frac{G_{dB}}{20}} \rightarrow A \approx 0.891$$

Then

$$0.891 = \frac{X - 2e^{Y}\left(1 + \frac{x^2}{2}\right)}{X}$$

$$\frac{X}{X - e^{Y}\left(1 + \frac{x^2}{2}\right)} = 1.122 \quad (53)$$

In most operating conditions, Y remains below zero. However, as its value approaches the origin, especially for small V_{DS} conditions, the excitation amplitude x associated with the 1 dB compression level decreases.

8.2. Two-Tone Intermodulation Testing

In narrowband amplifiers, nonlinearity can be characterized using a two-tone intermodulation test, in which two input signals of equal amplitude and slightly offset frequencies are introduced at the input stage. This process aims to identify the specific terms responsible for the intermodulation products produced by the amplifier. The stage size should be selected according to Equation (3) using the g_m/I_D design approach. Subsequently, the drain current I_D is obtained from (2).

The Voltage V_{GS} is given by $V_{GS} = V_{GS0} + V_{gm} cos(\omega_1 t) + V_{gm} cos(\omega_2 t)$. By applying the normalization approach outlined in Section IV, this expression can be rewritten accordingly. From Equation (7), assuming the device operates outside the saturation region, the relationship can be expressed ad

$$I_{out} = I_{ref}\left[\left(e^{\frac{V_{GS} - V_{TH}}{2n\phi_t}} + \frac{V_{GS} - V_{TH}}{2n\phi_t}\right)^2\right]$$

Using the normalization method described in Section IV, the resulting expression is as follows:

$$I_{out} = I_{ref}\left[\begin{pmatrix}\frac{V_{GS0} - V_{TH}}{2n\phi_t} + \frac{V_{gm}}{2n\phi_t} cos(\omega_1 t) + \\ \frac{V_{gm}}{2n\phi_t} cos(\omega_2 t) + e^{-\left(\frac{V_{GS0} - V_{TH}}{2n\phi_t} + \frac{V_{gm}}{2n\phi_t} cos(\omega_1 t) + \frac{V_{gm}}{2n\phi_t} cos(\omega_2 t)\right)}\end{pmatrix}^2\right]$$

$$I_{out} = I_{ref}\left[\begin{pmatrix}X + x\, cos(\omega_1 t) + \\ x\, cos(\omega_2 t) + e^{-(X + x\, cos(\omega_1 t) + x\, cos(\omega_2 t))}\end{pmatrix}^2\right] \quad (54)$$

The bias condition is selected such that (54) can be accurately approximated.

The exponential term is assumed to be insignificant. Therefore, the quadratic term is omitted, while the linear term is maintained because of its higher relevance.

$$I_{out} \approx I_{ref}\begin{bmatrix}(X + x\cos(\omega_1 t) + x\cos(\omega_2 t))^2 + \\ 2(X + x\cos(\omega_1 t) + x\cos(\omega_2 t))e^{-(X + x\cos(\omega_1 t) + x\cos(\omega_2 t))}\end{bmatrix} \tag{55}$$

At this point, the series expansion given in Equation (14) can be applied and rewritten in the following form, and to simplify the notation, the composite excitation signal is defined as

$$s(t) = X + x\cos(\omega_1 t) + x\cos(\omega_2 t)$$

Then

$$I_{out} \approx I_{ref}s(t)^2 + 2I_{ref}s(t)e^{-X}e^{-x\cos(\omega_1 t)}e^{-x\cos(\omega_2 t)}$$

$$I_{out} \approx I_{ref}s(t)^2 + 2I_{ref}s(t)e^{-X}[I_0(x) - 2I_1(x)\cos(\omega_1 t) + 2I_2(x)\cos(2\omega_1 t)]$$

$$\times [I_0(x) - 2I_1(x)\cos(\omega_2 t) + 2I_2(x)\cos(2\omega_2 t)] \tag{56}$$

Analyzing this expression makes it possible to determine the terms that dominate the intermodulation components. By expanding the expression and grouping these terms accordingly, we obtain the following outcome:

$$I_{out} \approx I_{ref}s(t)^2 + 2I_{ref}e^{-X}\big[XI_0{}^2(x) - 2XI_0(x)I_1(x)(\cos(\omega_1 t) + \cos(\omega_2 t))$$

$$+2XI_0(x)I_2(x)(\cos(2\omega_1 t) + \cos(2\omega_2 t)) + 4XI_1{}^2(x)\cos(\omega_1 t)\cos(\omega_2 t)$$

$$+4XI_2{}^2(x)\cos(2\omega_1 t)\cos(2\omega_2 t) - 4XI_1(x)I_2(x)(\cos(\omega_1 t)$$

$$\cos(2\omega_2 t) + \cos(2\omega_1 t)\cos(\omega_2 t)) + xI_0{}^2(x)\cos(\omega_1 t) - 2xI_0(x)I_1(x)$$

$$(2\cos(\omega_1 t)\cos(\omega_2 t) + \cos^2(\omega_1 t) + \cos^2(\omega_2 t)) + 2xI_0(x)I_2(x)$$

$$\big(\cos(\omega_1 t)(\cos(2\omega_2 t) + \cos(2\omega_1 t)) + \cos(\omega_2 t)(\cos(2\omega_2 t) + \cos(2\omega_1 t))\big)$$

$$+4xI_1{}^2(x)\cos(\omega_1 t)\cos(\omega_2 t)(\cos(\omega_1 t) + \cos(\omega_2 t)) + 4xI_2{}^2(x)\cos(2\omega_1 t)$$

$$\cos(2\omega_2 t)(\cos(\omega_1 t) + \cos(\omega_2 t)) - 4xI_1(x)I_2(x)(\cos^2(\omega_1 t)\cos(2\omega_2 t)$$

$$+\cos(\omega_1 t)\cos(2\omega_1 t)\cos(\omega_2 t) + \cos(\omega_1 t)\cos(2\omega_2 t)\cos(\omega_2 t) + \cos^2(\omega_2 t)\cos(2\omega_1 t)) + xI_0{}^2(x)\cos(\omega_2 t)\big]$$

We will concentrate on determining the intermodulation elements that have the biggest influence in the following stage. The investigation concentrated on third-order intermodulation products, which predominate the in-band distortions, and ignored higher-order intermodulation products because of their smaller amplitude and out-of-band position.

$$I_{out} \approx I_{ref}s(t)^2 + 2I_{ref}e^{-X}\big[4XI_1{}^2(x)\cos(\omega_1 t)\cos(\omega_2 t) - 4XI_1(x)I_2(x)$$

$$(\cos(\omega_1 t)\cos(2\omega_2 t) + \cos(2\omega_1 t)\cos(\omega_2 t)) - 4xI_0(x)$$

$$I_1(x)\cos(\omega_1 t)\cos(\omega_2 t) + 2xI_0(x)I_2(x)(\cos(\omega_1 t)\cos(2\omega_2 t) + \cos(\omega_2 t)\cos(2\omega_1 t))$$

$$+2xI_1{}^2(x)(\cos(2\omega_1 t)\cos(\omega_2 t) + \cos(\omega_1 t)\cos(2\omega_2 t)) + 2xI_2{}^2(x)$$

$$(\cos(2\omega_2 t)\cos(\omega_1 t) + \cos(2\omega_1 t)\cos(\omega_2 t)) - 2xI_1(x)I_2(x)$$

$$(\cos(\omega_1 t)\cos(2\omega_1 t) + \cos(\omega_1 t)\cos(2\omega_2 t))\big] \tag{57}$$

Equation (57) can be reformulated using Equation (12) as follows:

$$I_{out} \approx I_{ref}s(t)^2 + 2I_{ref}e^{-X}[x^2X\cos(\omega_1 t)\cos(\omega_2 t) + (1 - X)\frac{x^3}{4}(\cos(\omega_1 t)$$

$$\cos(2\omega_2 t) + \cos(2\omega_1 t)\cos(\omega_2 t)) - 2x^2\cos(\omega_1 t)\cos(\omega_2 t) + \frac{x^3}{2}$$

$$(\cos(2\omega_1 t)\cos(\omega_2 t) + \cos(\omega_1 t)\cos(2\omega_2 t)) + \frac{x^5}{32}$$

$$(\cos(2\omega_2 t)\cos(\omega_1 t) + \cos(2\omega_1 t)\cos(\omega_2 t)) - \frac{x^4}{8}$$

$$(cos(\omega_1 t) cos(2\omega_1 t) + cos(\omega_1 t) cos(2\omega_2 t))] \quad (58)$$

According to Equation (58), intermodulation components are eliminated when the bias condition $X = 1$, corresponding to $V_{GS0} - V_{TH} = 2n\phi_t$, is satisfied. However, analysis of this bias point suggests that operating precisely at this value is not recommended for designers. Instead, it is more effective to increase X, thereby moving into the strong inversion region, to reduce intermodulation effects. Moreover, the proposed nonlinear analysis approach has been successfully combined with the (g_m/I_D) design methodology.

9. Discussion and Conclusions

This research explores the nonlinear characteristics of MOSFET transistors using a physics-based simulation method that employs the BSIM4 model within the NGSpice simulation framework. Unlike simplified analytical approaches, the BSIM4 physical model provides a more precise depiction of nonlinear behaviors that manifest during actual device operation.

Such detail becomes particularly relevant in the moderate and strong inversion regions, where conventional approximations lose accuracy. Figure 4 illustrates the normalized drain current as a function of V_{GS} for three cosine input amplitudes at the gate of a 65nm MOSFET: 5mV, 3mV, and 2mV.

The signals are positioned within the moderate inversion range ($0.3V \leq V_{GS} \leq 1.0V$), enabling an analysis of how harmonic distortion changes in relation to the chosen bias point. From a theoretical perspective grounded in Bessel function analysis, the so-called "sweet points," where higher harmonic distortion is minimized or eliminated, should theoretically remain fixed regardless of the input signal's small amplitude. However, NGSpice simulations reveal that these points actually shift depending on the value of V_{GM}. Specifically, for $V_{GM} = 5mV$, the sweet points occur at $V_{GS} = 0.419V$ and $0.597V$; for 3mV, they shift to 0.423V and 0.545V; and for 2mV, they are found at 0.445V and 0.479V.

The shift toward the center of the moderate inversion region as V_{GM} decreases is due to lower amplitude signals covering a narrower range of V_{GS}. This causes their influence to be concentrated in the more linear portions of the device's response. Consequently, the points at which distortion is minimized correspond closely to the effective operating range of these signals. Contrary to the expectations derived from Bessel equations, simulation results reveal that harmonic components do not vanish entirely beyond the second sweet point; rather, they start to rise once more.

This behavior is attributed to the non-ideal characteristics captured by the NGSpice model, which incorporates physical phenomena including channel modulation, parasitic resistances, and variable carrier mobility, among other factors. In contrast to the original article, which includes a single graph due to the sweet points aligning across all three V_{GM} values, this study requires individual graphs for each V_{GM} Because the sweet points differ, there are six sweep points in total, two for each. V_{GM} making it necessary to present three separate graphs.

Each graph shows the normalized third harmonic amplitude of I_{DS} versus V_{GS}, considering different percentage tolerances in V_{TH}. Figure 6 suggests that. V_{GM} values ranging from 3mV to 5mV are the most appropriate. In contrast, the 2mV scenario, as shown by the NGSpice simulations, is deemed impractical for real-world applications. In summary, the NGSpice simulation confirms the anticipated performance of the MOSFET concerning the second harmonic. It reveals an operational range beginning at approximately. $V_{GS} = 0.6V$, within which the device exhibits notable linearization. However, addressing the third harmonic continues to be the main difficulty.Selecting NGSpice as the simulation tool was a key decision for this study.

As an open-source platform, it delivers a versatile and consistent environment for designing circuits while allowing direct manipulation of BSIM4 model parameters. This feature has made it possible to accurately set biasing conditions, device dimensions, and signal amplitudes critical for analyzing harmonics. Such precision is vital for examining effects like intermodulation distortion and harmonic generation, which play significant roles in amplifier design.

The findings show that it is possible to pinpoint operating points that reduce the second or third harmonic amplitudes by analyzing the drain current through Fourier methods, even without relying on intricate symbolic models. In addition, it can be observed how harmonics respond to variations in V_{TH} and other characteristics. BSIM4 is used because the model already naturally considers these factors.

This simulation-based approach offers a practical solution that complements specialized techniques such as the use of modified Bessel functions. Therefore, using BSIM4 in NGSpice allows for more accurate numerical verification of harmonic responses. This strategy incorporates second-order influences, including V_{DS} modulation, contact resistance, and mobility variations dependent on the electric field.

Conflicts of Interest

The authors declare that there is no conflict of interest regarding the publication of this paper.

Funding Statement

The authors declare that this research, as well as the resources used, were financed by themselves.

Acknowledgments

This work was undertaken by the authors, with guidance from their advisors and Dr. Fernando from the Federal University of Alagoas (UFAL) for their support during the development of this research. The authors also appreciate the feedback received from colleagues during the development of this manuscript.

References

[1] Yannis Tsividis, "Moderate Inversion in MOS Devices," *Solid-State Electronics*, vol. 25, no. 11, pp. 1099-1104, 1982. [CrossRef] [Google Scholar] [Publisher Link]

[2] Ronald Van Langevelde, and F.M. Klaasen, "Accurate Drain Conductance Modelling for Distortion Analysis in MOSFETs," *International Electron Devices Meeting. IEDM Technical Digest*, Washington, DC, USA, pp. 313-316, 1997. [CrossRef] [Google Scholar] [Publisher Link]

[3] B. Toole, C. Plett, and M. Cloutier, "RF Circuit Implications of Moderate Inversion Enhanced Linear Region in MOSFETs," *IEEE Transactions on Circuits and Systems I: Regular Papers*, vol. 51, no. 2, pp. 319-328, 2004. [CrossRef] [Google Scholar] [Publisher Link]

[4] Stephan C. Blaakmeer et al., "Wideband Balun-LNA with Simultaneous Output Balancing, Noise-Cancelling and Distortion-Cancelling," *IEEE Journal of Solid-State Circuits*, vol. 43, no. 6, pp. 1341-1350, 2008. [CrossRef] [Google Scholar] [Publisher Link]

[5] Jack Ou, and Farid Farahmand, "Transconductance/Drain Current based Distortion Analysis for Analog CMOS Integrated Circuits," *10th IEEE International NEWCAS Conference*, Montreal, QC, Canada, pp. 61-64, 2012. [CrossRef] [Google Scholar] [Publisher Link]

[6] Igor M. Filanovsky, and Luis B. Oliveira, "Using "Reconciliation" Model for Calculation of Harmonics in a MOS Transistor Stage Operating in Moderate Inversion," *2016 IEEE International Symposium on Circuits and Systems (ISCAS)*, Montreal, QC, Canada, pp. 474-477, 2016. [CrossRef] [Google Scholar] [Publisher Link]

[7] Y. Tsividis, K. Suyama, and K. Vavelidis, "Simple 'Reconciliation' MOSFET Model Valid in All Regions," *Electronics Letters*, vol. 31, no. 6, pp. 506-508, 1995. [CrossRef] [Google Scholar] [Publisher Link]

[8] Igor M. Filanovsky, J.K. Jarvenhaara, and Nikolay T. Tchamov, "On Moderate Inversion/Saturation Regions as Approximations to "Reconciliation" Model," *2016 IEEE Canadian Conference on Electrical and Computer Engineering (CCECE)*, Vancouver, BC, Canada, pp. 1-5, 2016. [CrossRef] [Google Scholar] [Publisher Link]

[9] Kenneth K. Clarke, and Donald T. Hess, *Communication Circuits: Analysis and Design*, Addison-Wesley, Reading, Massachusetts, 1971. [Google Scholar]

[10] David Binkley, *Tradeoffs and Optimization in Analog CMOS Design*, 1st Ed., John Wiley and xSons, 2008. [Google Scholar] [Publisher Link]

[11] Navid Paydavosi et al., "*BSIM4v4.8.0 MOSFET Model - User's Manual*," University of California, Berkeley, CA, USA, pp. 1-185, 2013. [Google Scholar]

[12] Holger Vogt et al., "*Ngspice User's Manual Version 44 (Ngspice Release Version)*," pp. 1-755, 2024. [Google Scholar]

[13] Igor M. Filanovsky, Luis B. Oliveira, and Nikolay T. Tchamov, "Using Modified Bessel Functions for Analysis of Nonlinear Effects in a MOS Transistor Operating in Moderate Inversion," *IEEE Transactions on Circuits and Systems I: Regular Papers*, vol. 66, no. 5, pp. 1897-1907, 2019. [CrossRef] [Google Scholar] [Publisher Link]

[14] Yannis Tsividis, and Colin McAndrew, *Operation and Modeling of the MOS Transistor*, 3rd ed., Oxford University Press, 2011. [Google Scholar] [Publisher Link]

[15] Elon Lages Lima, *Analysis Real*, IMCA, 1997. [Google Scholar]

[16] Norman William McLachlan, *Bessel Functions for Engineers*, 2nd ed., Clarendon Press, 1955. [Google Scholar]

Appendix 1

To complement the theoretical analysis, this section transitions the examination to an NGSpice simulation environment, aiming to verify whether the theoretical results are also reflected in a circuit simulation implementation. To achieve this, the SPICE and Python codes used are presented, along with the relevant circuit configurations and the resulting graphs. Comparing MATLAB with NGSpice offers a broader view of how the analytical expressions from the original work can be applied.

Definition of Parameters for the 65nm MOSFET:

For this study, a 65nm MOSFET transistor was utilized, with simulations conducted using NGSpice. The following are the fundamental parameters used for the simulation:

- Technology: 65 nm
- Threshold Voltage (V_{TH}): 0.24 V
- μC_{ox} (effective carrier mobility x oxide capacitance): $983 \mu A/V^2$
- Ideality Factor (n): 1.3

- Thermal Voltage (Vt): $25.9mV$
- Dimension Ratio (W/L): $50\mu m/0.36\mu m$
- Channel Length: 65 nm
- Transistor Type: NMOS

Netlist for MOSFET design in NGSpice:

This defines the key parameters used in the simulation of a 65 nm technology MOSFET for implementation in NGSpice using the BSIM4 model [11,12]. The values are matched to the model specifications and used in the Netlist to simulate the device.

- Threshold Voltage: Whit $V_{BS} = 0$, we have $V_{TH} = V_{TH0} = 0.24\,V$
- Effective carrier mobility for oxide capacitance:
  The low field mobility $\mu_0 = 0.0422\,m^2/(V \cdot s)$ is used. The oxide capacitance is estimated as:

$$C_{ox} = \frac{\varepsilon_{ox}}{TOXE}, \qquad \varepsilon_{ox} \approx 3.45 \times 10^{-11}$$

$$TOXE = 1.5 \times 10^{-9} \rightarrow C_{ox} \approx 0.023\,F/m^2$$

$$\mu C_{ox} \approx 0.0422 \times 0.023 = 971\,\mu A/V^2$$

- Ideality Factor (n):
  Using $C_{dep} = 1.228 \times 10^{-3}, C_{ox} = 0.023, \underline{n} = \frac{C_{dep}}{C_{ox}} \approx 0.0534$

$$NFACTOR = \frac{n-1}{\underline{n}} = \frac{0.3}{0.0534} \approx 5.62$$

- Thermal Voltage: $V_T = \frac{kT}{q} \approx 25.9\,mV$ at $300\,K$

Proof of the following equations:

Equation (3)

Transconductance corresponds to the rate of change of the drain current. I_D With respect to the Voltage V_{GS}, indicating how variations in V_{GS} affect the output current.

$$g_m = \frac{\partial I_D}{\partial V_{GS}}$$

The current I_D as the output current, we have

$$\frac{\partial I_D}{\partial V_{GS}} = \frac{\partial}{\partial V_{GS}}\left(I_{ref}\, ln^2\left(1 + e^{\frac{V_{GS}-V_{TH}}{2n\phi_t}}\right)\right)$$

Apply the chain rule. Derive I_{ref} with respect to the function $ln^2(u)$, and then u with respect to V_{GS}, where:

$$u = 1 + e^{\frac{V_{GS}-V_{TH}}{2n\phi_t}}$$

The derivate is expressed as:

$$\frac{\partial I_D}{\partial V_{GS}} = 2I_{ref}\, ln(u)\frac{1}{u}\frac{\partial u}{\partial V_{GS}}$$

Substitute u and $\partial u/\partial V_{GS}$ int o the expression

$$\frac{\partial I_D}{\partial V_{GS}} = 2I_{ref}\, ln\left(1+e^{\frac{V_{GS}-V_{TH}}{2n\phi_t}}\right)\frac{1}{1+e^{\frac{V_{GS}-V_{TH}}{2n\phi_t}}}\left(e^{\frac{V_{GS}-V_{TH}}{2n\phi_t}}\frac{1}{2n\phi_t}\right)$$

and, after making the corresponding simplifications, we obtain g_m

$$g_m = \frac{I_{ref}\, ln\left(1+e^{\frac{V_{GS}-V_{TH}}{2n\phi_t}}\right)e^{\frac{V_{GS}-V_{TH}}{2n\phi_t}}}{\left(1+e^{\frac{V_{GS}-V_{TH}}{2n\phi_t}}\right)n\phi_t}$$

from Equation (2)

$$I_D = I_{ref}\, ln^2\left(1+e^{\frac{V_{GS}-V_{TH}}{2n\phi_t}}\right)$$

$$\frac{I_D}{I_{ref}} = ln^2\left(1+e^{\frac{V_{GS}-V_{TH}}{2n\phi_t}}\right)$$

$$\sqrt{\frac{I_D}{I_{ref}}} = \left|ln\left(1+e^{\frac{V_{GS}-V_{TH}}{2n\phi_t}}\right)\right|$$

as $e^{\frac{V_{GS}-V_{TH}}{2n\phi_t}} > 0$, on the other hand, as $1+e^{\frac{V_{GS}-V_{TH}}{2n\phi_t}} > 1$, which implies that $\ln\left(1+e^{\frac{V_{GS}-V_{TH}}{2n\phi_t}}\right) > 0$, so that

$$\sqrt{\frac{I_D}{I_{ref}}} = ln\left(1+e^{\frac{V_{GS}-V_{TH}}{2n\phi_t}}\right)$$

$$e^{\sqrt{\frac{I_D}{I_{ref}}}} = 1+e^{\frac{V_{GS}-V_{TH}}{2n\phi_t}}$$

Replace in g_m

$$g_m = \frac{I_D\sqrt{\frac{I_{ref}}{I_D}}\left(e^{\sqrt{\frac{I_D}{I_{ref}}}}-1\right)}{e^{\sqrt{\frac{I_D}{I_{ref}}}}n\phi_t}$$

$$\frac{g_m}{I_D} = \frac{\sqrt{\frac{I_{ref}}{I_D}}}{n\phi_t}\left(\frac{e^{\sqrt{\frac{I_D}{I_{ref}}}}-1}{e^{\sqrt{\frac{I_D}{I_{ref}}}}}\right)$$

Equation (4)
Some useful propositions are introduced [15].
Proposition (Geometric series)
If $|x| < 1$, the sequence of partial sums $S_n = 1 + x + x^2 + \cdots + x^n$ converges, and

$$S_n = \sum_{n=0}^{\infty} x^n = \frac{1}{1-x}$$

If $|x| > 1$, the $\sum_{n=0}^{\infty} x^n$ series diverges.

Proposition: It is fulfilled

$$ln(1+x) = \sum_{n=1}^{\infty} \frac{(-1)^{n+1}(x)^n}{n}, |x| < 1$$

Now we proceed to find the equation.
Since $x > 1$, then $x - 1 > 0$, therefore

$$x = x$$

$$x = \frac{(x-1)x}{x-1}$$

$$ln(x) = ln\left(\frac{(x-1)x}{x-1}\right) = ln(x-1) + ln\left(\frac{x-1+1}{x-1}\right)$$

$$ln(x) = ln(x-1) + ln\left(1 + \frac{1}{x-1}\right)$$

$$ln(x) = ln(x-1) + \sum_{n=1}^{\infty} \frac{(-1)^{n+1}\left(\frac{1}{x-1}\right)^n}{n}$$

for $\left|\frac{1}{x-1}\right| < 1$, then $1 < |x-1|$.

Thus,

$$ln(x) = ln(x-1) + \sum_{n=1}^{\infty} \frac{(-1)^{n+1}}{(x-1)^n n}$$

$$ln(x) = ln(x-1) - \sum_{n=1}^{\infty} \frac{(-1)^n}{(x-1)^n n}, |x-1| > 1$$

then, $\ln^2(x)$

$$ln^2(x) = \left[ln(x-1) - \sum_{n=1}^{\infty} \frac{(-1)^n}{(x-1)^n n}\right]^2, |x-1| > 1$$

Equation (5)
Theorem (Infinitesimal Taylor's Formula) Let $f: I \to \mathbb{R}$ be n-times differentiable at the point $a \in I$. The function $r: J \to \mathbb{R}$, defined on the interval $J = \{h \in \mathbb{R} : a + h \in I\}$ by the equality

$$f(a+h) = f(a) + f'(a).h + \frac{f''(a)}{2!}.h^2 + \ldots + \frac{f^n(a)}{n!}.h^n + r(h),$$

satisfies $\lim_{h\to 0} \frac{r(h)}{h^n} = 0$. Conversely, if p(h) is a polynomial of degree $\leq n$ such that $r(h) = f(a+h) - p(h)$ satisfies $\lim_{h\to 0} \frac{r(h)}{h^n} = 0$, then p(h) is the Taylor polynomial of order n of f at the point a, that is [15],

$$p(h) = \sum_{i=0}^{n} \frac{f^{(i)}(a)}{i!} h^i.$$

Then, consider $h = x - a;\ f(x) = ln\ (x)$, and around the point $a\ =\ 1$

$$ln(\,x) = (x-1) - \frac{1}{2}(x-1)^2 + \frac{1}{3}(x-1)^3 - \cdots$$

$$ln(\,x) = \sum_{n=1}^{\infty} \frac{(-1)^{n+1}(x-1)^n}{n}$$

therefore, $ln^2(x)$

$$ln^2(\,x) = \left[\sum_{n=1}^{\infty} \frac{(-1)^{n+1}(x-1)^n}{n}\right]^2$$

The series converges on

$$|x-1| < 1$$

$$0 < x < 2$$

MATLAB Codes:
Figure 2

```
% Fixed parameters
VTH = 0.24;          % Threshold Voltage
n = 1.3;             % Substrate factor
phi_t = 0.0259;      % Thermal potential (in volts)

% Values of V_{gm} (small signal input) in millivolts
Vgm_values = [2e-3, 3e-3, 5e-3];

% Range of  V_{GS}  for the graph
VGS = linspace(0.25, 0.7, 800);

% Preassign A_3  for each value of  V_{gm}
A3_values = zeros(length(Vgm_values), length(VGS));

% Calculate A_3  for each V_{gm}
for j = 1:length(Vgm_values)
    Vgm = Vgm_values(j);
    for i = 1:length(VGS)
        % Calculate  X
        X = (VGS(i) - VTH) / (2 * n * phi_t);
        x=Vgm/(2 * n * phi_t);
        % Compute the modified Bessel functions
        I2 = besseli(2, x);
        I3 = besseli(3, x);

        % Calculate  A_3
        A3_values(j, i) = 2 * exp(-X) * (-2 * X*I3 + x * I2 - exp(-X) * besseli(3, 2*x));

    end
end
```

```
  % Plot the results
  figure;
  hold on;
  colors = {'b', 'r', 'k'}; % Assign colors for each curve
  for j = 1:length(Vgm_values)
      plot(VGS, abs(A3_values(j, :)), 'LineWidth', 0.5, 'Color', colors{j});
  end

  % Configure the graph
  grid on;
  xlabel('Gate-Source Voltage, V_{GS} (V)', 'FontSize', 12);
  ylabel('Harmonic amplitude, |A_3|', 'FontSize', 12);
  title('Normalized amplitude of the third harmonic', 'FontSize', 8);
  legend('V_{gm}=2mV', 'V_{gm}=3mV', 'V_{gm}=5mV', 'FontSize', 10, 'Location', 'northeast');
  xlim([0.25 0.7]);
hold off;
```

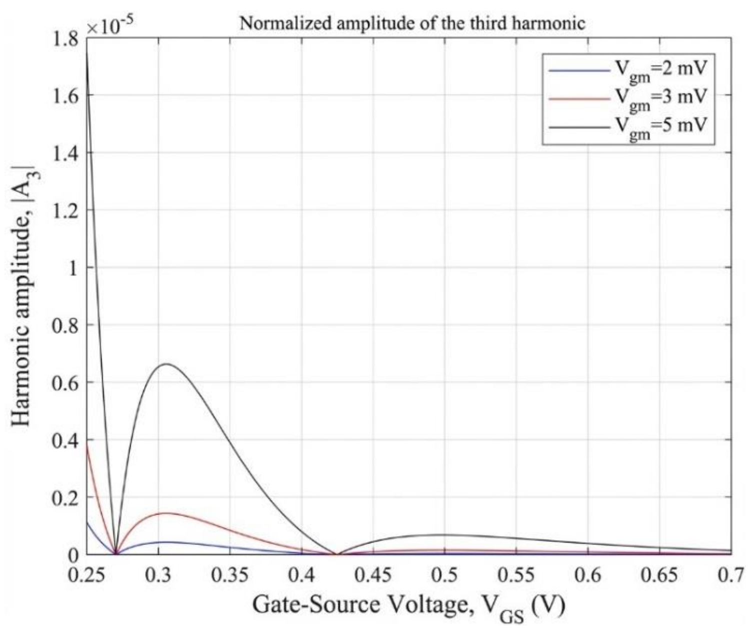

Figure 3

```
  % Fixed parameters
  VTH = 0.24;          % Threshold Voltage
  n = 1.3;             % Substrate factor
  phi_t = 0.0259;      % Thermal potential (in volts)

  % Values of V_{GS0}
  VGS_values = [0.264, 0.32, 0.37, 0.385, 0.420];
  %Tolerances
  tol=[0.1, 0.25, 0.5];
  % Range of V_{TH}  for the graph
  VTH_values=zeros(length(tol),800);
  for i=1:length(tol)
      VTH_values(i,:)= linspace(VTH-tol(i)*VTH, VTH+tol(i)*VTH, 800); % En volts
  end
  %Calculate  F3  for each value of  V_{GS0}
  X=zeros(length(VGS_values), length(VTH_values));
```

```
  F3_values = zeros(length(VGS_values), length(VTH_values));
  for i = 1:length(VGS_values)
     VGS = VGS_values(i);
     if i<3
        % Calculate  X
        X(i,:) = (VGS - VTH_values(i,:)) ./ (2 * n * phi_t);
        F3_values(i,:) = (exp(-X(i,:)) .* (- X(i,:) + 3 - 4*exp(-X(i,:))))/12;
     else
        X(i,:) = (VGS - VTH_values(end,:)) ./ (2 * n * phi_t);
        F3_values(i,:) = (exp(-X(i,:)) .* (- X(i,:) + 3 - 4*exp(-X(i,:))))/12;
       end
  end
  % Plot the results
  figure;
  hold on;
  lineStyles = {'-', '--', '-','-','--'}; % Line styles and markers
  colors = {'k', 'k', 'b', 'r', 'r'}; % Assign colors for each curve
  for j = 1:length(VGS_values)
     if j<3
        plot(VTH_values(j,:), abs(F3_values(j, :)), 'LineStyle',lineStyles{j}, 'LineWidth', 0.5, 'Color', colors{j});
     else
        plot(VTH_values(end,:), abs(F3_values(j, :)), 'LineStyle',lineStyles{j}, 'LineWidth', 0.5, 'Color', colors{j});
     end
  end
  % Configure the graph
  grid on;
  xlabel('Threshold Voltage, V_{TH} (V)', 'FontSize', 12);
  ylabel('|F_3|', 'FontSize', 12);
  title('Third harmonic distortion factor,|F_3(X)|', 'FontSize', 8);
  legend('V_{GS0}=0.264V,VTHtol=10%','V_{GS0}=0.32V,VTHtol=25%','V_{GS0}=0.37V,VTHtol=50%','V_{GS0}=0.38
  5V,VTHtol=50%',' V_{GS0}=0.420V,VTHtol=50%', 'FontSize', 10, 'Location', 'northwest');
  xlim([0.1 0.4]);
  ylim([0 0.09]);
hold off;
```

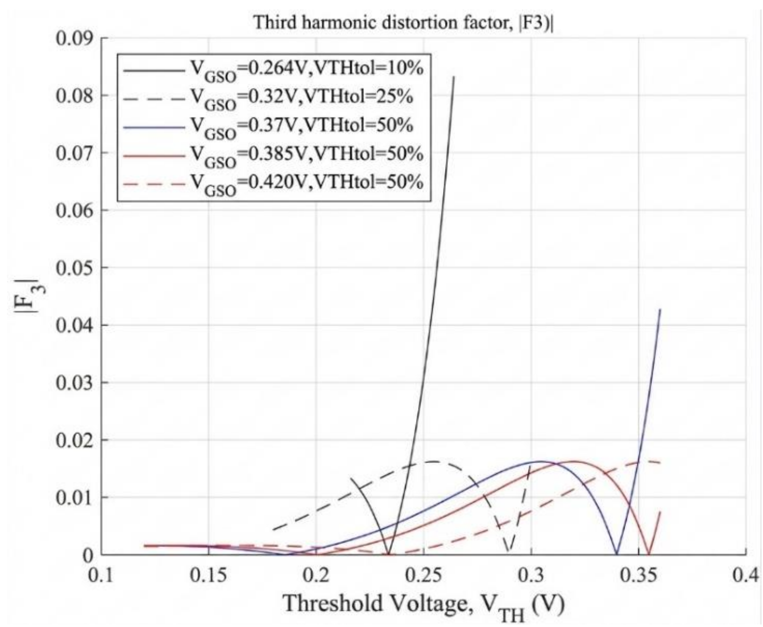

Figure 4

```
  % Fixed parameters
  VTH = 0.24;         % Threshold Voltage
  n = 1.3;            % Substrate factor
  phi_t = 0.0259;     % Thermal potential (in volts)

  % Values of V_{gm} (small signal input) in millivolts
  Vgm_values = [2e-3, 4e-3, 6e-3,8e-3];

  % Range of  V_{GS}  for the graph
  VGS = linspace(0.25, 0.5, 800);

  % Preassign A_2  for each value of  V_{gm}
  A2_values = zeros(length(Vgm_values), length(VGS));

  % Calculate A_2  for each V_{gm}
  for j = 1:length(Vgm_values)
     Vgm = Vgm_values(j);
     for i = 1:length(VGS)
        % Calculate  X
        X = (VGS(i) - VTH) / (2 * n * phi_t);
        x=Vgm/(2 * n * phi_t);
        % Compute the modified Bessel functions
        I1 = besseli(1, x);
        I2 = besseli(2, x);
        I3 = besseli(3, x);
         % Calculate  A_2  according to the given equation.
         A2_values(j, i) = x^2/2+2 * exp(-X) * (2 * X*I2 -x*(I1+I3)+ exp(-X) * besseli(2, 2*x));
     end
  end

  % Plot the results
  figure;
  hold on;
  colors = {'k', 'g', 'b', 'r'}; % Assign colors for each curve
  for j = 1:length(Vgm_values)
     plot(VGS, abs(A2_values(j, :)), 'LineWidth', 0.5, 'Color', colors{j});
  end

  % Configure the graph
  grid on;
  xlabel('Gate-Source Voltage, V_{GS} (V)', 'FontSize', 12);
  ylabel('Harmonic amplitude, |A_2|', 'FontSize', 12);
  title('Normalized amplitude of the second harmonic', 'FontSize', 8);
  leg=legend('V_{gm}=2mV', 'V_{gm}=4mV', 'V_{gm}=6mV',' V_{gm}=8mV', 'FontSize', 10, 'Location', 'northeast');
  pos=leg.Position;
  pos(2)=pos(2)-0.08;
  leg.Position=pos;
  xlim([0.25 0.5]);
hold off;
```

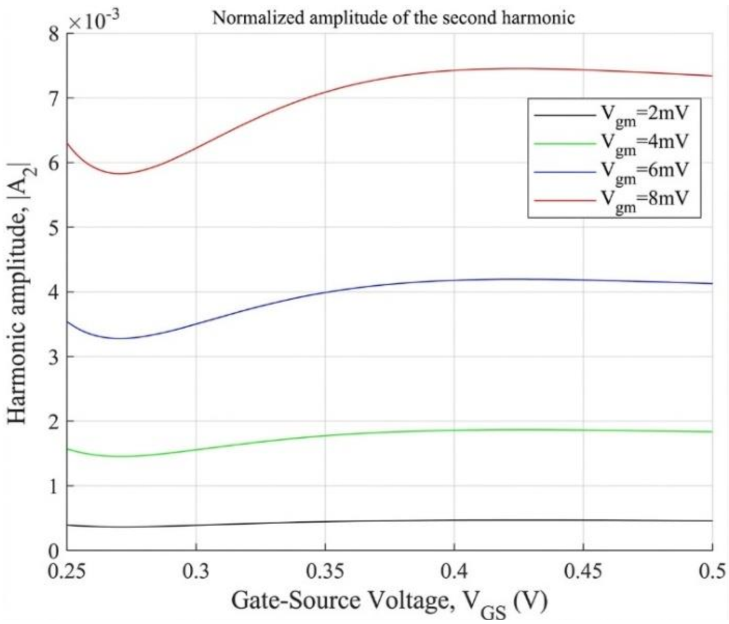

Figure 5

```
%Fixed parameters
VTH = 0.24;         % Threshold Voltage
n = 1.3;            % Substrate factor
phi_t = 0.0259;     % Thermal potential (in volts)

% Values of V_{GS0}
VGS_values = [0.264, 0.32, 0.37, 0.385, 0.420];
%Tolerances
tol=[0.1, 0.25, 0.5];
% Range of V_{TH}  for the graph
VTH_values=zeros(length(tol),800);
for i=1:length(tol)
    VTH_values(i,:)= linspace(VTH-tol(i)*VTH, VTH+tol(i)*VTH, 800);
end
%Calculate  F2  for each value of  V_{GS0}
X=zeros(length(VGS_values), length(VTH_values));
F2_values = zeros(length(VGS_values), length(VTH_values));
for i = 1:length(VGS_values)
    VGS = VGS_values(i);
    if i<3
        % Calculate  X
        X(i,:) = (VGS - VTH_values(i,:)) / (2 * n * phi_t);
        F2_values(i,:) = 1/2*(1+exp(-X(i,:)) .* ( X(i,:) - 2*(1-exp(-X(i,:)))));
    else
        X(i,:) = (VGS - VTH_values(end,:)) / (2 * n * phi_t);
        F2_values(i,:) = 1/2*(1+exp(-X(i,:)) .* ( X(i,:) - 2*(1-exp(-X(i,:)))));

     end
end
% Plot the results
figure;
hold on;
lineStyles = {'-', '--', '-','-','--'}; % Line styles and markers
colors = {'k', 'k', 'b', 'r', 'r'}; % Assign colors for each curve
```

```
  for j = 1:length(VGS_values)
     if j<3
        plot(VTH_values(j,:), F2_values(j, :),'LineStyle',lineStyles{j}, 'LineWidth', 0.5,'Color', colors{j});
     else
        plot(VTH_values(end,:),F2_values(j, :), 'LineStyle',lineStyles{j}, 'LineWidth', 0.5, 'Color', colors{j});
     end
  end
  % Configure the graph
  grid on;
  xlabel('Threshold Voltage, V_{TH} (V)', 'FontSize', 12);
  ylabel('F_2(X)', 'FontSize', 12);
  title('Second harmonic distortion factor F_2(X) ', 'FontSize', 8);
  leg=legend('V_{GS0}=0.264V,VTHtol=10%', 'V_{GS0}=0.32V,VTHtol=25%',
  'V_{GS0}=0.37V,VTHtol=50%','V_{GS0}=0.385V,VTHtol=50%','V_{GS0}=0.420V,VTHtol=50%', 'FontSize', 8,
  'Location', 'northwest');
  pos=leg.Position;
  pos(2)=pos(2)-0.3;
  leg.Position=pos;
  xlim([0.1 0.4]);
hold off;
```

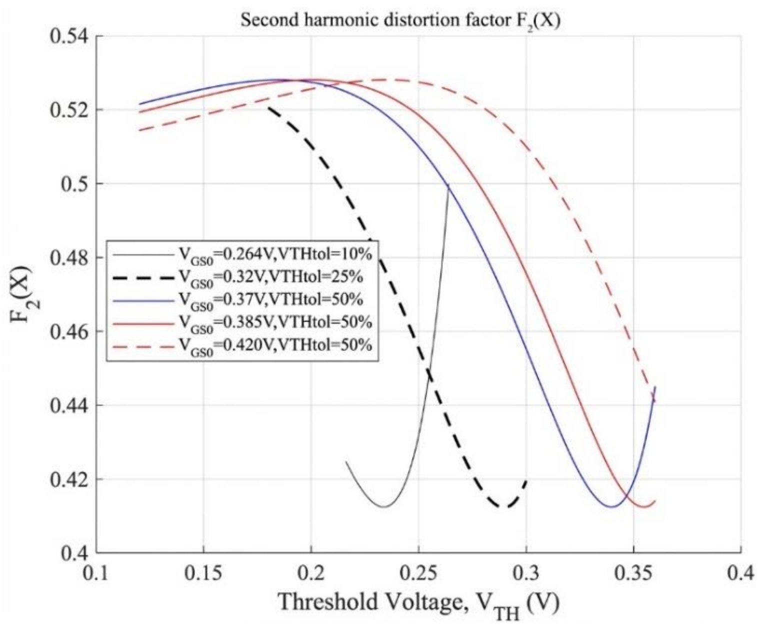

Figure 6

```
  % Fixed parameters
  VTH = 0.24;          % Threshold Voltage
  n = 1.3;             % Substrate factor
  phi_t = 0.0259;      % Thermal potential (in volts)
  % Values of V_{gm} (small signal input) in millivolts
  Vgm_values = 2e-3;
  Iz=238;%238uA
  % Range of  V_{GS}  for the graph
  VGS = linspace(0.25, 0.7, 983);
  % Preassign A_3  for each value of  V_{gm}
  A3_values = zeros(1, length(VGS));
  % Calculate A_3  for each V_{gm}
  for i = 1:length(VGS)
     % Calculate  X
```

```
      X = (VGS(i) - VTH) / (2 * n * phi_t);
      x=Vgm_values/(2 * n * phi_t);
      % Compute the modified Bessel functions
      I2 = besseli(2, x);
      I3 = besseli(3, x);
      %  Calculate  A_3
      A3_values(1, i) = 2 * exp(-X) * (-2 * X*I3 + x * I2 - exp(-X) * besseli(3, 2*x));
      %A3*Iz(238uA)
      I3_values=A3_values*Iz;
  end
  figure;
  plot(VGS, abs(A3_values), 'k', 'LineWidth', 0.5);
  hold on;
  % Configure the graph
  grid on;
  xlabel('Gate-Source Voltage, V_{GS} (V)', 'FontSize', 12);
  ylabel('Amplitude of the third harmonic, uA', 'FontSize', 12);
  title('Normalized amplitude of the third harmonic', 'FontSize', 8);
  legend('Calculated', 'Simulated', 'FontSize', 10, 'Location', 'northeast');
  xlim([0.2 0.7]);
hold off;
```

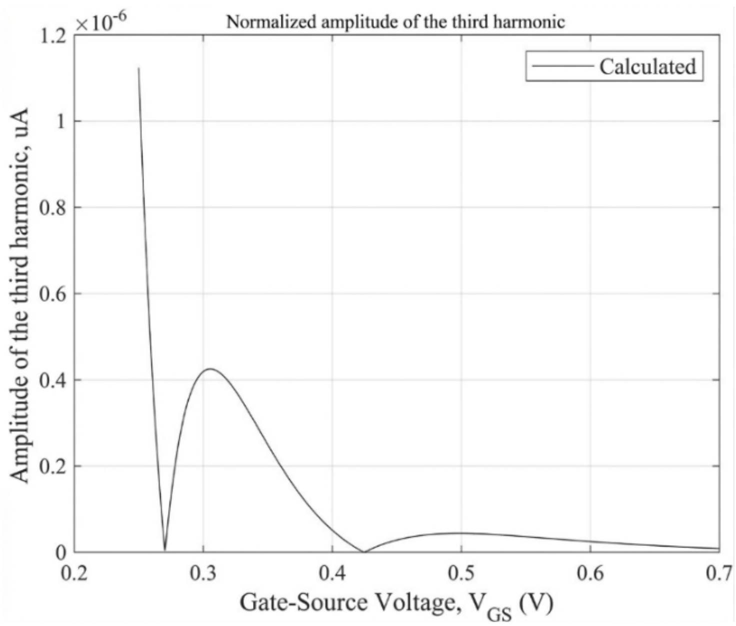

Figure 8

```
  % Fixed parameters
  VTH = 0.24;          % Threshold Voltage
  n = 1.3;             % Substrate factor
  phi_t = 0.0259;      % Thermal potential (in volts)
  Vgm_values=5e-3;
  Vdm_values=5e-3;
  VDS_values=[0.2, 0.3, 0.4];
  % Range of V_{GS}
  VGS = linspace(0.3, 0.5, 800);
  % Defining the dimensions
  X=zeros(length(VDS_values), length(VGS));
  Y=zeros(length(VDS_values), length(VGS));
  A3_values = zeros(length(VDS_values), length(VGS));
```

```
 B3_values = zeros(length(VDS_values), length(VGS));
 D3_values = zeros(length(VDS_values), length(VGS));
 IMH_values = zeros(length(VDS_values), length(VGS));
 x=Vgm_values/(2 * n * phi_t);
 y=Vdm_values/(phi_t);
  for i = 1:length(VDS_values)
      VDS=VDS_values(i);
      for j=1:length(VGS)
         X(i,j) = (VGS(1,j) - VTH) / (2 * n * phi_t);
         Y(i,j) = (VGS(1,j) - VTH-n*VDS) / (n * phi_t);
         %A3
         I2 = besseli(2, x);
         I3 = besseli(3, x);
         %A3_values(i, j) = 2 * exp(-X(i,j)) .* (-2 * X(i,j)*I3 + x * I2 - exp(-X(i,j)) * besseli(3, 2*x));
         A3_values(i,j) = x^3* (exp(-X(i,j)).*(- X(i,j) + 3 - 4*exp(-X(i,j))))/12;
         %B3
         B3_values(i,j)=-exp(Y(i,j))*x^3/3;
         %D3
         D3_values(i,j) =exp(Y(i,j)) * (2 * besseli(3, y)*besseli(0,2*x));
         %IMH
         IMH_values(i,j) =2* exp(Y(i,j)) * besseli(1, 2*x)*besseli(1,y);
      end
     figure(i)
     semilogy(VGS, abs(A3_values(i, :)),'k--', 'LineWidth', 0.5);
     hold on;
     semilogy(VGS, abs(B3_values(i, :)), 'r', 'LineWidth', 0.5);
     semilogy(VGS, abs(D3_values(i, :)),'b-', 'LineWidth', 0.5);
     semilogy(VGS, abs(IMH_values(i, :)),'k-', 'LineWidth', 0.5);
     grid on;
     xlabel('Gate-Source Voltage, V_{GS} (V)', 'FontSize', 12);
     ylabel('Normalized amplitude', 'FontSize', 12);
     title('Third harmonic and intermodulation', 'FontSize', 8);
     legend('A_{3}', 'B_{3}', 'D_{3}',' IMH_{W-w}', 'FontSize', 10, 'Location', 'southeast');
     hold off;
end
```

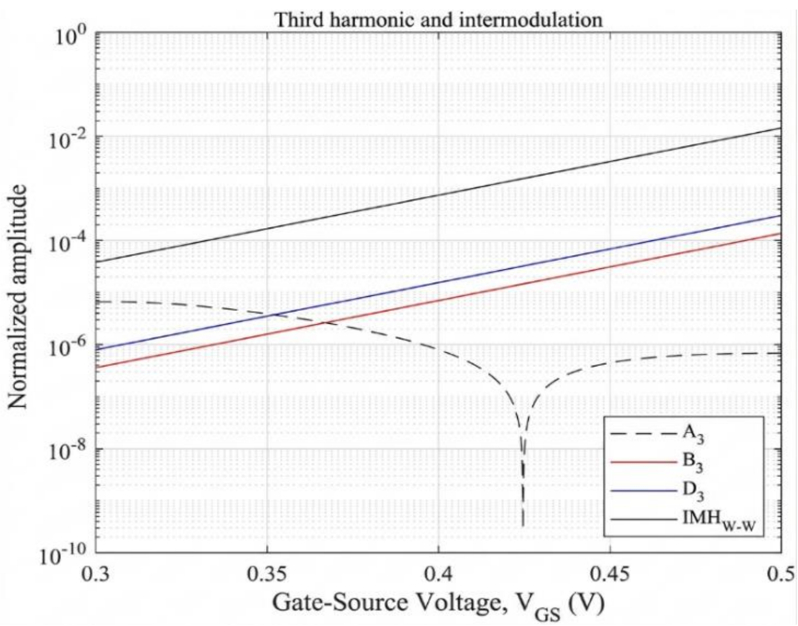

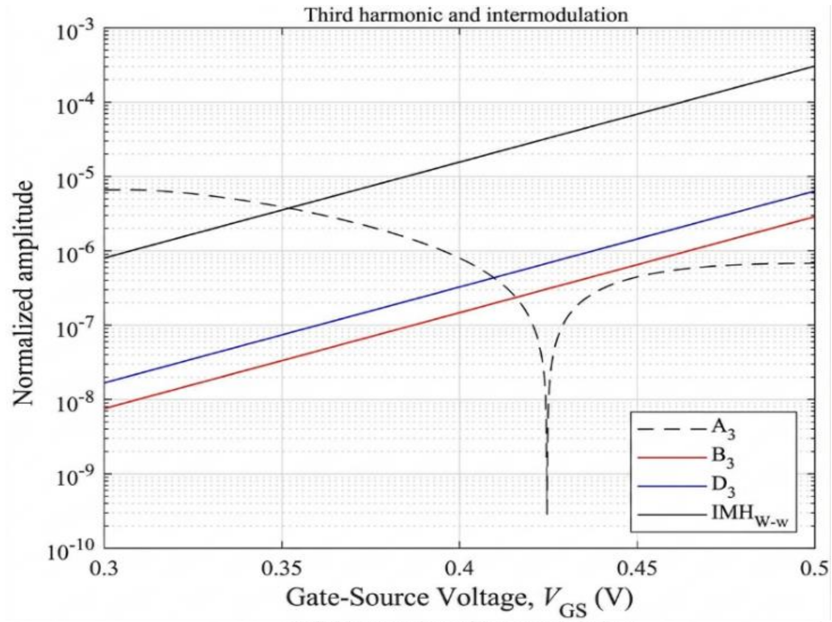

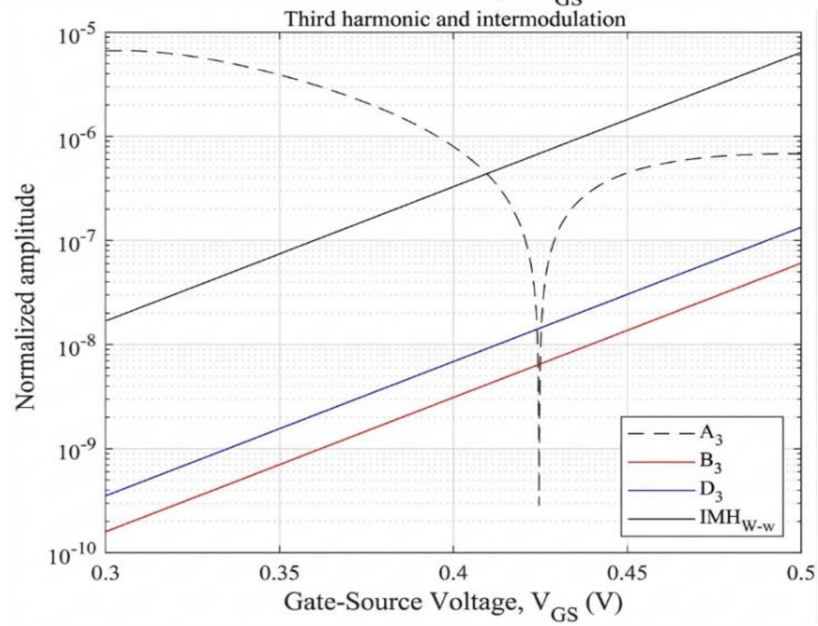

Appendix 2

NGSPICE Codes

This section presents the drain current I_{DS} and energy curves as functions of time, obtained through simulations in Ngspice. These curves allow validation of the threshold voltage value (V_{TH}) of the transistor.

$I_{DS}\ vs\ Time\ curves$

```
*Simulation of ID-VDS Curves of the MOSFET
.option savecurrents_bsim4; Save the Drain Current of the BSIM4 MOSFET
.model nmos_65nm nmos level=14 version=4.8 vth0=0.24 u0=0.0422 NFACTOR=5.62 TOXE=1.5e-9 w=50u l=0.36u
Vgs_DC 1 0 DC 0.4            ; DC Power Supply for Gates
Vds_DC 4 0 DC 1              ; Drain Source
Vgs_AC 1 2 SIN(0 5m 1k 0 0 90)   ; AC Cosine Power Supply with 5mV and 1kHz
R1 4 3 1
M1 3 2 0 0 nmos_65nm w=50u l=0.36u   ; MOSFET: D=3, G=2, S=0, B=0
.option savecurrents; Record All Currents in the Circuit
```

```
  .save i(R1) ;Log Current through R1
  .probe I(R1) ;Log Current through R1
  .control
     *dc Vds_DC 0 1.5 0.01 Vgs_DC 0.14 0.64 0.1 ;Nested Double Sweep
     dc Vgs_DC 0 1 0.01
     *wrdata NGS_id_vds.txt i(R1)
     wrdata NGS_id_vgs.txt i(R1)
     plot i(R1)
     *dc Vgs_DC 0 1 0.01
     *let ID = i(R1)
     *let gm = deriv(ID)
     *plot gm
     *print xval(gm, max(gm))
  .endc
.end
```

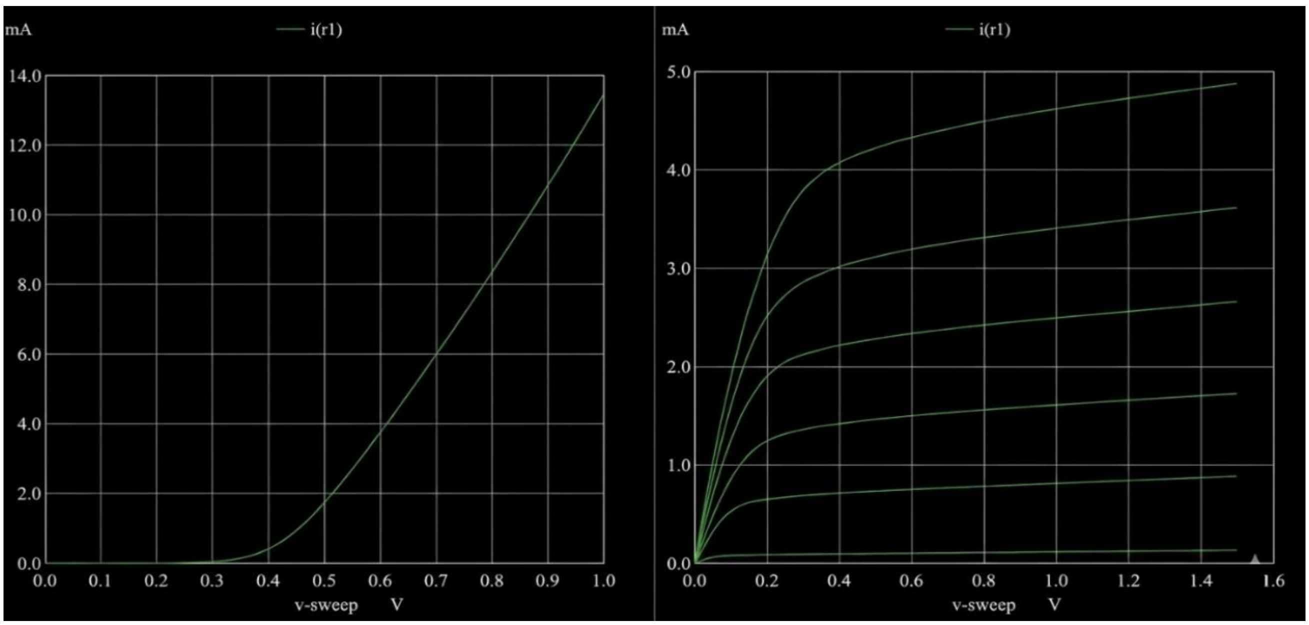

In the figure on the left, it can be seen that as the gate voltage. V_{GS} increases, the drain current I_{DS} remains at zero until a certain threshold value is reached. This point, where I_{DS} begins to increase significantly, is defined as the threshold voltage V_{TH}. This value indicates the onset of conduction in the MOSFET channel, signifying the transition from the cutoff region to the triode or linear region. The figure on the right illustrates a sweep of the drain voltage. V_{DS} versus the drain current I_{DS}, with distinct curves corresponding to various values of V_{GS}.

Harmonics

```
  FINAL_MOSFET_SECONDVERSION
  .option savecurrents_bsim4
  .model nmos_65nm nmos level=14 version=4.8 vth0=0.24 u0=0.0422 NFACTOR=5.62 TOXE=1.5e-9 w=25u l=0.18u
  Vgs_DC 1 0 DC 0.1
  Vgs_AC 1 2 SIN(0 2m 1k 0 0 90); Here, the Vgm (amplitude of the sine wave) is changed.
  Vds_DC 4 0 DC 1
  R1 4 3 1
  M1 3 2 0 0 nmos_65nm W=25u L=0.18u
  .option savecurrents
  .save I(R1)
  .probe I(R1)
  .tran 0.05m 50m
```

```
 .control
    ; Define parameters for the sweep.
    let VgsDC_start = 0.1
    let VgsDC_end   = 2
    let num_steps   = 513
    let VgsDC_step  = {(VgsDC_end - VgsDC_start) / (num_steps - 1)}
    let fft_results = vector(num_steps)  ; Create a vector with 800 elements.
    let step_num    = 0
    let vgsdc_current = VgsDC_start
    ; Loop to execute the simulation at each step.
    dowhile step_num < num_steps
       alter Vgs_DC dc = vgsdc_current    ; Update the source with the current value.
       run                                ; Run the simulation.
       linearize i(R1)                    ; Linearize the current.
       fft I(R1)                          ; Calculate the FFT of I(R1).
       let fft_magnitud = mag(i(R1))             ; Store the magnitude of the FFT
       let valor_save = fft_magnitud[154]      ; index 154 -> 3khz, 52 -> 1khz, 102 -> 2khz
       let fft_results[step_num] = valor_save ; Store the value in the vector
       let vgsdc_current = vgsdc_current + VgsDC_step  ; Proceed to the next value
       let step_num = step_num + 1                    ; Increment the counter
    end
    let fft_matrix = fft_results
    ; Optional: Print the matrix to confirm its structure.
    print fft_matrix
    Save the complete matrix in a .txt file.
    wrdata NGS_2vgm_3k_25-018.txt fft_matrix
 .endc
.end

 SWEEP_VTH_MOSFET
 .option savecurrents_bsim4
 .model nmos_65nm nmos level=14 version=4.8 vth0=0.24 u0=0.0422 NFACTOR=5.62 TOXE=1.5e-9 w=50u l=0.36u
 Vgs_DC 1 0 DC 0.541; Adjust based on the target Vgs
 Vgs_AC 1 2 SIN(0 3m 1k 0 0 90)
 Vds_DC 4 0 DC 1
 R1 4 3 1
 M1 3 2 0 0 nmos_65nm W=50u L=0.36u
 .option savecurrents
 .save I(R1)
 .probe I(R1)
 .tran 0.05m 50m
 .control
    ; Setup for the sweep at VTH0
    let VTH0_start = 0.12 ;-X% de Vth
    let VTH0_end   = 0.36 ;+X% de vth
    let num_steps  = 513
    let VTH0_step  = {(VTH0_end - VTH0_start) / (num_steps - 1)}
    let fft_results = vector(num_steps)
    let step_num = 0
    let vth0_current = VTH0_start
    dowhile step_num < num_steps
       altermod nmos_65nm vth0 = vth0_current
       run
       linearize i(R1)
       fft i(R1)
       let fft_magnitud = mag(i(R1))
```

```
        let valor_save = fft_magnitud[154] ; index 154 -> 3khz, 52 -> 1khz, 102 -> 2khz
        let fft_results[step_num] = valor_save
        let vth0_current = vth0_current + VTH0_step
        let step_num = step_num + 1
    end
    let fft_matrix = fft_results
    print fft_matrix
    wrdata NGS_3vgm_0541vgs_3k.txt fft_matrix
  .endc
.end
```

Appendix 3

Data Processing and Visualization with Python

Below are the Python codes used to process and visualize the data obtained from the simulations conducted in NGSpice. These data were previously exported in .txt format, and their processing is essential for clearly and comprehensibly visualizing the results. This stage complements the simulation presented in the previous subsection.

Drain Current

```
  import numpy as np
  import matplotlib.pyplot as plt
  def cargar_bloques(filename):
    datos = np.loadtxt(filename, comments=['*', '#'])
    v, i = datos[:, 0], datos[:, 1]
    bloques_v = []
    bloques_i = []
    # Detect increases in voltage (when it subsequently decreases - new curve)
    inicio = 0
    for j in range(1, len(v)):
        if v[j] < v[j-1]:
            bloques_v.append(v[inicio:j])
            bloques_i.append(i[inicio:j])
            inicio = j
    # Incorporate the final block
    bloques_v.append(v[inicio:])
    bloques_i.append(i[inicio:])
    return bloques_v, bloques_i
  # Input Files
  archivo1 = 'NGS_id_vds.txt'
  archivo2 = 'NGS_id_vgs.txt'
  # Load individual curves
  v1_bloques, i1_bloques = cargar_bloques(archivo1)
  v2_bloques, i2_bloques = cargar_bloques(archivo2)

  # Generate plot
  plt.figure(figsize=(8, 6))

  # File 1 (without offset)
  for v, i in zip(v1_bloques, i1_bloques):
    plt.plot(v, i, color='blue', label='Curva 1' if 'Curva 1' not in plt.gca().get_legend_handles_labels()[1] else "")

  # File 2 (with an X offset of -0.24 V)
  for v, i in zip(v2_bloques, i2_bloques):
    v_desplazada = v - 0.24  # Subtract 0.24 V from all X-axis values
    plt.plot(v_desplazada, i, color='red', linestyle='--', label='Curva 2 (desplazada)' if 'Curva 2 (desplazada)' not in plt.gca().get_legend_handles_labels()[1] else "")
  plt.xlabel('Voltage (V)')
```

```
  plt.ylabel('Current (A)')
  plt.title('I-V Curves from Two Files (Curve 2 Offset on the X-axis)')
  plt.grid(True)
  plt.legend()
  plt.tight_layout()
plt.show()
```

Figure 2

```
  import numpy as np
  import matplotlib.pyplot as plt

  # Function to Read the Second Column of the File
  def extraer_magnitudes(nombre_archivo):
      data = np.loadtxt(nombre_archivo)
      return data[:, 1]  # Retorna solo la segunda columna

  # Define the Files for Each Vgm
  archivos = {
      "5mV": ("NGS_5vgm_1k.txt", "NGS_5vgm_3k.txt"),
      "3mV": ("NGS_3vgm_1k.txt", "NGS_3vgm_3k.txt"),
      "2mV": ("NGS_2vgm_1k.txt", "NGS_2vgm_3k.txt")
  }

  # Dictionary for Storing Calculated Ratios
  razones = {}

  # Process Each File Set
  for Vgm, (archivo_1k, archivo_3k) in archivos.items():
      magnitudes_1k = extraer_magnitudes(archivo_1k)
      magnitudes_3k = extraer_magnitudes(archivo_3k)

      # Ensure Both Vectors Contain 513 Values
      if len(magnitudes_1k) != 513 or len(magnitudes_3k) != 513:
          raise ValueError(f"The {Vgm} Files Do Not Contain 513 Values Each. Please Verify the Content.)

      # Calculate the Ratio of Magnitudes
      razones[Vgm] = magnitudes_3k / magnitudes_1k

  # Generate the X-axis (VgsDC) with 513 Values Ranging from 0.1 to 2
  num_steps = 513
  VgsDC = np.linspace(0.1, 2, num_steps)


  # Plot the Data
  plt.figure(figsize=(8, 5))

  plt.plot(VgsDC, razones["5mV"], 'r-', linewidth=1.2, label="Vgm = 5mV")
  plt.plot(VgsDC, razones["3mV"], 'b-', linewidth=1.2, label="Vgm = 3mV")
  plt.plot(VgsDC, razones["2mV"], 'k-', linewidth=1.2, label="Vgm = 2mV")

  # Graph Configuration
  plt.xlabel("Gate-Source Voltage, Vgs, V")
  plt.ylabel("Harmonic Amplitude, |A3|")
  plt.title("Normalized third harmonic amplitude")
  plt.legend()
  plt.grid(True)
```

```
  #Display the Graph
plt.show()
```

Figure 3

```
import numpy as np
import matplotlib.pyplot as plt

# Function to Read and Extract the Second Column from a File
def extraer_columna_derecha(nombre_archivo):
    with open(nombre_archivo, "r") as file:
        data = [float(line.strip().split()[1]) for line in file if len(line.strip().split()) >= 2]
    return np.array(data)

# Files Organized by Each Vgs0
archivos = {
    "0.445": ("NGS_2vgm_0445vgs_1k.txt", "NGS_2vgm_0445vgs_3k.txt"),
    "0.500": ("NGS_2vgm_05vgs_1k.txt", "NGS_2vgm_05vgs_3k.txt"),
    "0.545": ("NGS_2vgm_0545vgs_1k.txt", "NGS_2vgm_0545vgs_3k.txt"),
    "0.566": ("NGS_2vgm_0566vgs_1k.txt", "NGS_2vgm_0566vgs_3k.txt"),
    "0.576": ("NGS_2vgm_0576vgs_1k.txt", "NGS_2vgm_0576vgs_3k.txt"),
}

# Custom VTH Ranges for Each Vgs0
rangos_VTH = {
    "0.445": (0.216, 0.264),
    "0.500": (0.18, 0.30),
    "0.545": (0.12, 0.36),
    "0.566": (0.12, 0.36),
    "0.576": (0.12, 0.36),
}

# Line Styles and Labels
estilos = {
    "0.445": ('k-', "V_gs0=0.445V, VTHtol=10%"),
    "0.500": ('k--', "V_gs0=0.500V, VTHtol=25%"),
    "0.545": ('b-', "V_gs0=0.545V, VTHtol=50%"),
    "0.566": ('r-', "V_gs0=0.566V, VTHtol=50%"),
    "0.576": ('r--', "V_gs0=0.576V, VTHtol=50%"),
}
plt.figure(figsize=(10, 6))
for Vgs0, (archivo_1k, archivo_3k) in archivos.items():
    datos_1k = extraer_columna_derecha(archivo_1k)
    datos_3k = extraer_columna_derecha(archivo_3k)
    if len(datos_1k) != 513 or len(datos_3k) != 513:
        raise ValueError(f"Files for Vgs0={Vgs0} do not contain 513 values.")
    razon = datos_3k / datos_1k
    vth_min, vth_max = rangos_VTH[Vgs0]
    VTH = np.linspace(vth_min, vth_max, 513)
    estilo_linea, etiqueta = estilos[Vgs0]
    plt.plot(VTH, razon, estilo_linea, linewidth=1.5, label=etiqueta)

# Graph Configuration
plt.xlabel("Threshold Voltage, Vth, V")
plt.ylabel("Harmonic Amplitude |F3|")
```

```
  plt.title("Third harmonic distortion factor, Vgm=2mV")
  plt.xlim(0.1, 0.4)
  plt.grid(True)
  plt.legend()
  plt.tight_layout()
plt.show()
```

Figure 4

```
  import numpy as np
  import matplotlib.pyplot as plt

  # Function to Read and Extract Interleaved Values from a File
  def extraer_magnitudes(nombre_archivo):
      with open(nombre_archivo, "r") as file:
          data = np.array(file.readline().split(), dtype=float)  # Leer y convertir en array de floats
      return data[1::2]  # Extraer cada segundo valor desde el indice 1

  # Define the Files for Each Vgm (Now at 2 kHz and 1 kHz)
  archivos = {
      "2mV": ("ulti_2vgm_1k.txt", "ulti_2vgm_2k.txt"),
      "4mV": ("ulti_4vgm_1k.txt", "ulti_4vgm_2k.txt"),
      "6mV": ("ulti_6vgm_1k.txt", "ulti_6vgm_2k.txt"),
      "8mV": ("ulti_8vgm_1k.txt", "ulti_8vgm_2k.txt")
  }

  # Dictionary for Storing Calculated Ratios
  razones = {}

  # Process Each Set of Files
  for Vgm, (archivo_1k, archivo_2k) in archivos.items():
      magnitudes_1k = extraer_magnitudes(archivo_1k)
      magnitudes_2k = extraer_magnitudes(archivo_2k)

      # Ensure Both Vectors Contain 800 Values
      if len(magnitudes_1k) != 800 or len(magnitudes_2k) != 800:
          raise ValueError(f"The {Vgm} Files Do Not Contain 800 Values Each. Please Verify the Content.")

      # Calculate the Magnitude Ratio
      razones[Vgm] = magnitudes_2k / magnitudes_1k

  # Create the X-axis (VgsDC) with 800 Values Ranging from 0.1 to 3
  num_steps = 800
  VgsDC = np.linspace(0.1, 3, num_steps)
  # Plot the Data
  plt.figure(figsize=(8, 5))

  plt.plot(VgsDC, razones["2mV"], 'k-', linewidth=1.2, label="Vgm = 2mV")
  plt.plot(VgsDC, razones["4mV"], 'g-', linewidth=1.2, label="Vgm = 4mV")
  plt.plot(VgsDC, razones["6mV"], 'b-', linewidth=1.2, label="Vgm = 6mV")
  plt.plot(VgsDC, razones["8mV"], 'r-', linewidth=1.2, label="Vgm = 8mV")

  # Graph Configuration
  plt.xlabel("VgsDC (V)")
  plt.ylabel("Magnitude Ratio (2kHz / 1kHz)")
  plt.title("Magnitude Ratio as a Function of VgsDC for Various Vgm")
  plt.legend()
```

```
  plt.grid(True)

  # Display the Graph
plt.show()
```

Figure 6

```
  import numpy as np
  import matplotlib.pyplot as plt

  # Read the Second Column from a Two-Column File
  def extraer_magnitudes(nombre_archivo):
      data = np.loadtxt(nombre_archivo)
      return data[:, 1]  # Second Column

  # Read a File with Only a Single Column
  def extraer_magnitudes_columna(nombre_archivo):
      with open(nombre_archivo, "r") as file:
          data = np.array([float(line.strip()) for line in file.readlines()])
      return data

  # Files
  archivo_3k = "NGS_2vgm_3k.txt"
  archivo_amplitud = "A3_amplitud_3.txt"  # Este tiene solo una columna

  # Load Data
  magnitudes_3k = extraer_magnitudes(archivo_3k)
  magnitudes_amplitud = extraer_magnitudes_columna(archivo_amplitud)

  # Validation
  if len(magnitudes_3k) != 513 or len(magnitudes_amplitud) != 513:
      raise ValueError("One of the Files Does Not Contain 513 Values. Please Verify the Content.")

  # X-axis
  VgsDC = np.linspace(0.1, 2, 513)

  # Plot the Data
  plt.figure(figsize=(8, 5))

  plt.plot(VgsDC, magnitudes_3k, 'k-', linewidth=1.2, label="simulada")
  plt.plot(VgsDC, magnitudes_amplitud, 'r-', linewidth=1.2, label="calculada")
  #
  plt.xlabel("Gate-Source Voltage, Vgs, V")
  plt.ylabel("Third Harmonic Amplitude, A")
  plt.title("Third Harmonic Amplitude")
  plt.legend()
  plt.grid(True)
plt.show()
```

Figure 7

```
  import numpy as np
  import matplotlib.pyplot as plt

  # Function to extract the second column from a two-column file
  def extraer_segunda_columna(nombre_archivo):
      data = np.loadtxt(nombre_archivo)
      return data[:, 1]  # Segunda columna
```

```
  # Directly specify the file names
  archivo_1 = "NGS_2vgm_3k_25-018.txt"
  archivo_2 = "NGS_2vgm_3k_50-036.txt"

  # Import data
  magnitudes_1 = extraer_segunda_columna(archivo_1)
  magnitudes_2 = extraer_segunda_columna(archivo_2)

  # Validation process
  if len(magnitudes_1) != 513 or len(magnitudes_2) != 513:
      raise ValueError("One of the files lacks 513 entries in its second column. Please verify its contents.")

  # X-axis representation
  VgsDC = np.linspace(0.1, 2, 513)

  # Graphing
  plt.figure(figsize=(8, 5))

  plt.plot(VgsDC, magnitudes_1, 'b-', linewidth=1.5, label="W/L = 25um/0.18um")
  plt.plot(VgsDC, magnitudes_2, 'r-', linewidth=1.5, label="W/L = 50um/0.36um")

  # Visual appeal
  plt.xlabel("Gate-Source Voltage, Vgs (V)")
  plt.ylabel("Third Armonic Amplitde, A")
  plt.title("Third Armonic Amplitde")
  plt.legend()
  plt.grid(True)
  plt.tight_layout()
plt.show()
```